Electronic Supplementary Material (ESI) for Dalton Transactions.
This journal is © The Royal Society of Chemistry 2016

Electronic Supplementary Information (ESI) for:

Synthesis, characterization, and gas-phase fragmentation of rhenium–carbonyl complexes bearing imidazol(in)ium-2-dithiocarboxylate ligands

Tomás F. Beltrán,[a] Guillermo Zaragoza,[b] and Lionel Delaude[*a]

[a]*Laboratory of Organometallic Chemistry and Homogeneous Catalysis, Institut de chimie (B6a), Allée du six Août 13, Quartier Agora, Université de Liège, 4000 Liège, Belgium*

[b]*Unidade de Difracción de Raios X, Edificio CACTUS, Universidade de Santiago de Compostela, Campus Vida, 15782 Santiago de Compostela, Spain*

Table of content

Part 1 - Experimental Procedures

1. General Information

All the reactions were carried out using standard Schlenk techniques under a dry argon atmosphere. Solvents were distilled from appropriate drying agents and deoxygenated prior to use. Rhenium(I) pentacarbonyl bromide, decacarbonyldirhenium(0), and sodium-mercury amalgam (4–5% Na) were purchased from Strem. The NHC·CS_2 zwitterions were prepared according to literature.[1] Unless otherwise specified, ^{1}H and ^{13}C{^{1}H} NMR spectra were recorded at 273 or 298 K with a Bruker DRX 400 spectrometer. Chemical shifts are listed in parts per million downfield from TMS and are referenced from the solvent peaks or TMS. Electrospray mass spectra were obtained using a Micromass LCT Premier instrument. Infrared spectra were recorded with a Bruker Equinox 55 FT–IR spectrometer. Elemental analyses were carried out in the Laboratory of Pharmaceutical Chemistry at the University of Liège.

2. Synthesis of Mononuclear [$ReBr(CO)_3(S_2C{\cdot}NHC)$] Complexes

A 50 mL two-neck round-bottomed flask equipped with a magnetic stirring bar and a three-way stopcock was loaded with [$ReBr(CO)_5$] (40.6 mg, 0.100 mmol) and a NHC·CS_2 zwitterion (0.105 mmol). The reactor was purged of air by applying three vacuum/argon cycles before dry toluene (15 mL) was added. The reaction mixture was heated in an oil bath at 120 ºC for 1 h leading to a dark colored suspension, which was cooled to room temperature and filtered with suction. The precipitate was washed with toluene (5 mL) and *n*-pentane (10 mL). It was dried under high vacuum to afford complexes **1**–**5**.

[$ReBr(CO)_3(S_2C{\cdot}ICy)$] (1). Orange microcrystalline solid (0.0489 g, 74% yield). ^{1}H NMR (400 MHz, CD_2Cl_2, 273 K): δ 1.20–1.23 (m, 2 H, Cy), 1.51–1.63 (m, 8 H, Cy), 1.74–1.77 (br d, 2 H, Cy), 1.87–1.90 (br d, 4 H, Cy), 2.15–2.18 (br d, 4 H, Cy), 4.79 (m, 2 H, CHN Cy), 7.28 ppm (s, 2 H, =CHN). ^{13}C NMR (100 MHz CD_2Cl_2, 273 K): δ 25.0 (CH_2), 25.3 (CH_2), 34.0 (CH_2), 59.2 (CHN), 118.4 (Im-$C^{4,5}$), 147.4 (Im-C^2), 187.3 (CO), 193.9 (CO), 225.9 ppm (CS_2). IR (KBr): ν_{CO} 2015 (s), 1914 (s), 1896 (s) cm^{-1}. ESI-MS (CH_3CN) *m/z*: calcd for $C_{19}H_{24}N_2O_3ReS_2$ ([M–Br]$^+$), 579.0786; found, 579.0780. Anal. calcd for $C_{19}H_{24}BrN_2O_3ReS_2$ (658.65): C, 34.65; H, 3.67; N, 4.25; S, 9.74. Found: C, 37.49; H, 3.93; N, 4.07; S, 9.33.

[$ReBr(CO)_3(S_2C{\cdot}IMes)$] (2). Dark purple microcrystalline solid (0.0458 g, 63% yield). ^{1}H NMR (400 MHz, CD_2Cl_2, 273 K): δ 2.16 (s, 12 H, *ortho*-CH_3), 2.39 (s, 6 H, *para*-CH_3), 7.09 (s, 4 H,

meta-CH), 7.37 ppm (s, 2 H, =CHN). ^{13}C NMR (100 MHz, CD_2Cl_2, 273 K): δ 18.2 (CH_3), 21.5 (CH_3), 124.4 (Im-$C^{4,5}$), 130.2 (CH_{ar}), 130.9 (C_{ar}), 135.1 (C_{ar}), 142.4 (C_{ar}), 144.4 (Im-C^2), 186.6 (CO), 193.7 (CO), 220.4 ppm (CS_2). IR (KBr): ν_{CO} 2016 (s), 1924 (s), 1898 (s) cm^{-1}. ESI-MS (CH_3CN, 20 V) *m/z*: calcd for $C_{25}H_{24}N_2O_3ReS_2$ ([M–Br]$^+$), 651.0786; found, 651.0767. Anal. calcd for $C_{25}H_{24}BrN_2O_3ReS_2$ (730.71): C, 41.09; H, 3.31; N, 3.83; S, 8.78. Found: C, 38.66; H, 3.14; N, 3.68; S, 9.45.

[ReBr(CO)$_3$(S$_2$C·IDip)] (3). Dark purple microcrystalline solid (0.0553 g, 68% yield). ^{1}H NMR (400 MHz, CD_2Cl_2, 298 K): δ 1.21 (d, $^3J_{H,H}$ = 6.8 Hz, 12 H, CH(C*H*$_3$)$_2$), 1.38 (d, $^3J_{H,H}$ = 6.8 Hz, 12 H, CH(C*H*$_3$)$_2$), 2.49 (sept, $^3J_{H,H}$ = 6.8 Hz, 4 H, C*H*(CH$_3$)$_2$), 7.38 (s, 2 H, =CHN), 7.41 (br s, 4 H, *meta*-CH), 7.63 ppm (t, $^3J_{H,H}$ = 7.6 Hz, 2 H, *para*-CH). ^{13}C NMR (100 MHz, CD_2Cl_2, 298 K): δ 23.0 (CH_3), 25.7 (CH_3), 30.2 ((CH$_3$)$_2$*C*H), 125.3 (Im-$C^{4,5}$), 125.6 (CH_{ar}), 131.0 (C_{ar}), 132.9 (CH_{ar}), 145.7 (C_{ar}), 146.1 (Im-C^2), 186.2 (CO), 193.7 (CO), 219.4 ppm (CS_2). IR (KBr): ν_{CO} 2013 (s), 1924 (s), 1895 (s) cm^{-1}. ESI-MS (CH_3CN, 20 V) *m/z*: calcd for $C_{31}H_{36}N_2O_3ReS_2$ ([M–Br]$^+$), 735.1725; found, 735.1718. Anal. calcd for $C_{31}H_{36}BrN_2O_3ReS_2$ (814.87): C, 45.69; H, 4.45; N, 3.44; S, 7.87. Found: C, 45.72; H, 4.46; N, 3.55; S, 7.58.

[ReBr(CO)$_3$(S$_2$C·SIMes)] (4). Dark purple microcrystalline solid (0.0606 g, 83% yield). ^{1}H NMR (400 MHz, CD_2Cl_2, 298 K): δ 2.33 (s, 6 H, *para*-CH_3), 2.42 (s, 12 H, *ortho*-CH_3), 4.29 (s, 4 H, CH_2), 7.02 ppm (s, 4 H, *meta*-CH). ^{13}C NMR (100 MHz, CD_2Cl_2, 298 K): δ 18.6 (CH_3), 21.5 (CH_3), 51.1 (CH_2N), 130.7 (C_{ar}), 130.8 (C_{ar}), 136.0 (C_{ar}), 141.6 (C_{ar}), 163.6 (Im-C^2), 186.3 (CO), 193.8 (CO), 221.6 ppm (CS_2). IR (KBr): ν_{CO} 2018 (s), 1926 (s), 1891 (s) cm^{-1}. ESI-MS (CH_3CN, 20 V) *m/z*: calcd for $C_{25}H_{26}N_2O_3ReS_2$ ([M–Br]$^+$), 653.0942; found, 653.0933. Anal. calcd for $C_{25}H_{26}BrN_2O_3ReS_2$ (732.71): C, 40.98; H, 3.58; N, 3.82; S, 8.75. Found: C, 40.97; H, 3.56; N, 3.94; S, 8.89.

[ReBr(CO)$_3$(S$_2$C·SIDip)] (5). Dark purple microcrystalline solid (0.0707 g, 87% yield). ^{1}H NMR (400 MHz, CD_2Cl_2, 298 K): δ 1.34 (d, $^3J_{H,H}$ = 8.0 Hz, 12 H, CH(C*H*$_3$)$_2$), 1.45 (d, $^3J_{H,H}$ = 8.0 Hz, 12 H, CH(C*H*$_3$)$_2$), 3.07 [sept, $^3J_{H,H}$ = 8.0 Hz, 4 H, C*H*(CH$_3$)$_2$), 4.35 (s, 4 H, CH_2), 7.32 (d, $^3J_{H,H}$ = 8.0 Hz, 4 H, *meta*-CH), 7.52 ppm (t, $^3J_{H,H}$ = 8.0 Hz, 2 H, *para*-CH). ^{13}C NMR (100 MHz, CD_2Cl_2, 298 K): δ 23.7 (CH_3), 26.7 (CH_3), 30.1 ((CH$_3$)$_2$*C*H), 53.2 (CH_2N), 125.8 (CH_{ar}), 130.5 (C_{ar}), 132.0 (CH_{ar}), 146.7 (C_{ar}), 178.1 (Im-C^2), 187.6 (CO), 193.6 (CO), 217.7 ppm (CS_2). IR (KBr): ν_{CO} 2016 (s), 1930 (s), 1895 (s) cm^{-1}. ESI-MS (CH_3CN) *m/z*: calcd for $C_{31}H_{38}N_2O_3ReS_2$ ([M–Br]$^+$),

737.1881; found, 737.1877. Anal. cald for $C_{31}H_{38}BrN_2O_3ReS_2$ (816.88): C, 45.58; H, 4.69; N, 3.43; S, 7.85. Found: C, 44.64; H, 4.56; N, 3.45; S, 7.77.

3. Synthesis of Binuclear $[Re_2(CO)_8(S_2C{\cdot}NHC)]$ Complexes

A solution of $Na[Re(CO)_5]$ was prepared by stirring a mixture of $Re_2(CO)_{10}$ (0.036 g, 0.055 mmol) and an excess of Na(Hg) amalgam (4–5 weight-% of Na, 0.1560 g, 6 equiv.) in dry THF (15 mL) for 40 min at room temperature. The yellow-colored supernatant solution was transferred with a cannula into a slurry of a $[ReBr(CO)_3(S_2C{\cdot}NHC)]$ complex (0.1 mmol) in dry THF (5 mL). The reaction mixture was stirred at room temperature for 1 h. After evaporation of the solvent in vacuo, the residue was taken up with dichloromethane (5 mL) and filtered through a short plug of Celite. The inorganic salts were rinsed with dichloromethane (2 × 2 mL) and the filtrate was slowly poured into *n*-pentane (80 mL) under vigorous stirring. The precipitate was filtered with suction and washed with *n*-pentane (2 × 10 mL). It was dried under high vacuum to afford complexes **6**–**8**.

$[Re_2(CO)_8(S_2C{\cdot}ICy)]$ (6). Brown microcrystalline solid (0.061 g, 67% yield). ^{1}H NMR (400 MHz, CD_2Cl_2, 273 K): δ 1.20–1.25 (m, 2 H, Cy), 1.36–1.46 (m, 8 H, Cy), 1.53–1.65 (m, 2 H, Cy), 1.82–1.91 (br d, 4 H, Cy), 2.13–2.17 (br d, 4 H, Cy), 5.15 (m, 2 H, CHN Cy), 7.19 ppm (s, 2 H, =CHN). ^{13}C NMR (100 MHz CD_2Cl_2, 298 K): δ 25.1 (CH_2), 25.4 (CH_2), 33.8 (CH_2), 59.1 (CHN), 118.4 (Im-$C^{4,5}$), 149.9 (Im-C^2), 193.3 (2 CO), 200.2 (2 CO), 208.6 (4 CO), 216.7 ppm (CS_2). IR (KBr): ν_{CO} 2079 (m), 2013 (s), 1986 (s), 1969 (s), 1940 (s), 1895 (s) cm^{-1}. ESI-MS ($C_2H_4Cl_2$) *m/z*: calcd for $C_{24}H_{24}N_2O_8Re_2S_2$ ([M]$^+$), 906.0089; found, 906.0077. Anal. calcd for $C_{24}H_{24}N_2O_8Re_2S_2$ (905.02): C, 31.85; H, 2.67; N, 3.10; S, 7.09. Found: C, 30.56; H, 3.02; N, 3.06; S, 6.89.

$[Re_2(CO)_8(S_2C{\cdot}IMes)]$ (7). Reddish-brown microcrystalline solid (0.0684 g, 70% yield). ^{1}H NMR (400 MHz, CD_2Cl_2, 273 K): δ 2.11 (s, 12 H, *ortho*-CH_3), 2.33 (s, 6 H, *para*-CH_3), 7.01 (s, 4 H, *meta*-CH), 7.36 ppm (s, 2 H, =CHN). ^{13}C NMR (100 MHz, CD_2Cl_2, 273 K): δ 18.3 (CH_3), 21.3 (CH_3), 123.5 (C_{ar}), 130.0 (C_{ar}), 130.5 (C_{ar}), 135.1 (C_{ar}), 142.1 (C_{ar}), 152.1 (Im-C^2), 193.5 (2 CO), 200.9 (2 CO), 207.5 (4 CO), 212.2 ppm (CS_2). IR (KBr): ν_{CO} 2063 (m), 2007 (s), 1958 (s), 1927 (s), 1908 (s), 1884 (s) cm^{-1}. ESI-MS ($C_2H_4Cl_2$) *m/z*: calcd for $C_{30}H_{24}N_2O_8Re_2S_2$ ([M]$^+$), 978.0089; found, 978.0078. Anal. calcd for $C_{30}H_{24}N_2O_8Re_2S_2$ (977.06): C, 36.88; H, 2.48; N, 2.87; S, 6.56. Found: C, 36.19; H, 2.61; N, 3.10; S, 7.27.

[$Re_2(CO)_8(S_2C{\cdot}IDip)$] (8). Brown microcrystalline solid (0.0400 g, 38% yield). ^{1}H NMR (400 MHz, CD_2Cl_2, 273 K): δ 1.14 (d, $^3J_{H,H}$ = 8.0 Hz, 12 H, CH(CH_3)$_2$), 1.31 (d, $^3J_{H,H}$ = 8.0 Hz, 12 H, CH(CH_3)$_2$), 2.51 (sept, $^3J_{H,H}$ = 8.0 Hz, 4 H, CH(CH$_3$)$_2$), 7.32 (d, $^3J_{H,H}$ = 8.0 Hz, 4 H, *meta*-CH), 7.36 (s, 2 H, =CHN), 7.55 ppm (t, $^3J_{H,H}$ = 8.0 Hz, 2 H, *para*-CH). ^{13}C NMR (100 MHz, CD_2Cl_2, 273 K): δ 22.2 (CH$_3$), 26.4 (CH$_3$), 30.0 ((CH$_3$)$_2$*C*H), 124.1 (Im-C^{4,5}), 125.2 (C$_{ar}$), 129.3 (C$_{ar}$), 132.6 (C$_{ar}$), 145.7 (C$_{ar}$), 152.7 (Im-C^2), 193.2 (2 CO), 200.5 (2 CO), 207.1 (4 CO), 213.7 ppm (CS$_2$). IR (KBr) ν_{CO} 2062 (m), 2007 (s), 1961 (s), 1939 (s), 1924 (s), 1895 (s) cm^{-1}. ESI-MS ($C_2H_4Cl_2$) *m/z*: calcd for $C_{36}H_{36}N_2O_8Re_2S_2$ ([M]$^+$), 1062.1028; found, 1062.1094. Anal. calcd for $C_{36}H_{36}N_2O_8Re_2S_2$ (1061.22): C, 40.74; H, 3.42; N, 2.64; S, 6.04. Found: C, 40.55; H, 3.64; N, 2.79; S, 6.02.

4. Synthesis of Binuclear [$Re_2(CO)_6(S_2C{\cdot}NHC)$] Complexes

A solution of Na[Re(CO)$_5$] was prepared by stirring a mixture of $Re_2(CO)_{10}$ (0.036 g, 0.055 mmol) and an excess of Na(Hg) amalgam (4–5 weight-% of Na, 0.1560 g, 6 equiv.) in dry THF (15 mL) for 40 min at room temperature. The yellow-colored supernatant solution was transferred with a cannula into a slurry of [ReBr(CO)$_3$($S_2C{\cdot}$SIMes)] (**4**, 73.1 mg, 0.1 mmol) or [ReBr(CO)$_3$-($S_2C{\cdot}$SIDip)] (**5**, 81.7 mg, 0.1 mmol) in dry THF (5 mL). The reaction mixture was heated in an oil bath at 60 ºC for 1.5 h. After evaporation of the solvent in vacuo, the residue was taken up with dichloromethane (5 mL) and filtered through a short plug of Celite. The inorganic salts were rinsed with dichloromethane (2 × 2 mL) and the filtrate was slowly poured into *n*-pentane (80 mL) under vigorous stirring. The precipitate was filtered with suction and washed with *n*-pentane (2 × 10 mL). It was dried under high vacuum to afford complexes **9** and **10**.

[$Re_2(CO)_6(S_2C{\cdot}$SIMes)] (9). Brown microcrystalline solid (0.0320 g, 35% yield). ^{1}H NMR (400 MHz, CD_2Cl_2, 298 K): δ 2.31 (s, 6 H, *para*-CH$_3$), 2.39 (s, 12 H, *ortho*-CH$_3$), 3.92 (4, 2 H, CH$_2$), 6.99 ppm (s, 4 H, *meta*-CH). ^{13}C NMR (100 MHz, CD_2Cl_2, 298 K): δ 18.6 (CH$_3$), 21.3 (CH$_3$), 50.8 (CH$_2$N), 79.0 (CS$_2$), 130.6 (C$_{ar}$), 130.9 (C$_{ar}$), 135.6 (C$_{ar}$), 140.8 (C$_{ar}$), 172.4 (Im-C^2), 191.4 (CO), 196.0 (CO). IR (KBr): ν_{CO} 2026 (s), 1995 (s), 1911 (br s), 1889 (s) cm^{-1}. ESI-MS ($C_2H_4Cl_2$) *m/z*: calcd for $C_{28}H_{26}N_2O_6Re_2S_2$ ([M]$^+$), 924.0347; found, 924.0378. Anal. calcd for $C_{28}H_{26}N_2O_6Re_2S_2$ (923.06): C, 36.43; H, 2.84; N, 3.04; S 6.95. Found: C, 35.38; H, 2.77; N, 3.54; S, 6.84.

[$Re_2(CO)_6(S_2C{\cdot}$SIDip)] (10). Brown microcrystalline solid (0.0565 g, 56% yield) ^{1}H NMR (400 MHz, CD_2Cl_2, 273 K): δ 1.31 (d, $^3J_{H,H}$ = 8.0 Hz, 12 H, CH(CH_3)$_2$), 1.54 (d, $^3J_{H,H}$ = 8.0 Hz, 12 H, CH(CH_3)$_2$), 3.01 [sept, $^3J_{H,H}$ = 8.0 Hz, 4 H, CH(CH$_3$)$_2$), 4.02 (s, 4 H, CH$_2$), 7.30 (d, $^3J_{H,H}$ = 8.0 Hz,

4 H, *meta*-CH), 7.47 ppm (t, $^{3}J_{H,H}$ = 8.0 Hz, 2 H, *para*-CH). ^{13}C NMR (100 MHz, CD_2Cl_2, 273 K): δ 23.6 (CH_3), 26.3 (CH_3), 30.0 (($CH_3)_2CH$), 53.8 (CH_2N), 79.0 (CS_2), 125.5 (CH_{ar}), 131.2 (CH_{ar}), 133.5 (C_{ar}), 146.6 (C_{ar}), 175.0 (Im-C^2), 191.6 (CO), 195.8 (CO). IR (KBr) ν_{CO} 2026 (s), 1997 (s), 1933 (s), 1908 (s), 1883 (s) cm^{-1}. ESI-MS ($C_2H_4Cl_2$) *m/z*: calcd for $C_{34}H_{38}N_2O_6Re_2S_2$ ($[M]^+$), 1008.1287; found, 1008.1241. Anal. calcd for $C_{34}H_{38}N_2O_6Re_2S_2$ (1007.20): C, 40.54; H, 3.80; N, 2.78; S, 6.37. Found: C, 38.89; H, 3.42; N, 2.94; S, 6.28.

Synthesis of $[Re_2(CO)_6(S_2C{\cdot}IMes)]$ (11) and $[Re_2(CO)_6(S_2C{\cdot}IDip)]$ (12). A 50 mL two-neck round-bottomed flask equipped with a magnetic stirring bar and a three-way stopcock was loaded with $[Re_2(CO)_8(S_2C{\cdot}IMes)]$ (**7**, 45.1 mg, 0.050 mmol) or $[Re_2(CO)_8(S_2C{\cdot}IDip)]$ (**8**, 53.1 mg, 0.050 mmol). The reactor was purged of air by applying three vacuum/argon cycles before dry petroleum ether (bp 100–140 ºC, 10 mL) was added. The reaction mixture was heated in an oil bath at 130 ºC for 1 h, leading a yellow-colored suspension, which was cooled to room temperature and filtered with suction. The precipitate was washed with *n*-pentane (10 mL) and dried under high vacuum to afford complexes **11** and **12**.

$[Re_2(CO)_6(S_2C{\cdot}IMes)]$ (11). Yellowish-brown microcrystalline solid (0.0305 g, 66% yield). ^{1}H NMR (400 MHz, CD_2Cl_2, 298 K): δ 2.17 (s, 12 H, *ortho*-CH_3), 2.38 (s, 6 H, *para*-CH_3), 7.09 (s, 4 H, *meta*-CH), 7.12 ppm (s, 2 H, =CHN). ^{13}C NMR (100 MHz, CD_2Cl_2, 298 K): δ 18.6 (CH_3), 21.6 (CH_3), 79.3 (CS_2), 123.1 (Im-$C^{4,5}$), 130.6 (CH_{ar}), 131.6 (C_{ar}), 135.2 (C_{ar}), 142.3 (C_{ar}), 154.3 (Im-C^2), 192.0 (CO), 196.2 ppm (CO). IR (KBr): ν_{CO} 2023 (s), 1993 (s), 1923 (s), 1904 (s), 1889 (s) cm^{-1}. ESI-MS ($C_2H_4Cl_2$) *m/z*: calcd for $C_{28}H_{24}N_2O_6Re_2S_2$ ($[M]^+$), 922.0191; found, 922.0171. Anal. calcd for $C_{28}H_{24}N_2O_6Re_2S_2$ (921.04): C, 36.51; H, 2.63; N, 3.04; S, 6.96. Found: C, 35.29; H, 3.13; N, 2.61; S, 5.41.

$[Re_2(CO)_6(S_2C{\cdot}IDip)]$ (12). Brown microcrystalline solid (0.0352 g, 70% yield) ^{1}H NMR (400 MHz, CD_2Cl_2, 298 K): δ 1.18 (d, $^{3}J_{H,H}$ = 8.0 Hz, 12 H, $CH(CH_3)_2$), 1.48 (d, $^{3}J_{H,H}$ = 8.0 Hz, 12 H, $CH(CH_3)_2$), 2.53 (sept, $^{3}J_{H,H}$ = 8.0 Hz, 4 H, $CH(CH_3)_2$), 7.16 (s, 2 H, =CHN), 7.38 (d, $^{3}J_{H,H}$ = 8.0 Hz, 4 H, *meta*-CH),7.58 ppm (t, $^{3}J_{H,H}$ = 8.0 Hz, 2 H, *para*-CH). ^{13}C NMR (100 MHz, CD_2Cl_2, 298 K): δ 22.8 (CH_3), 25.5 (CH_3), 30.1 (($CH_3)_2CH$), 79.0 (CS_2), 124.1 (Im-$C^{4,5}$), 125.3 (C_{ar}), 131.7 (C_{ar}), 132.4 (C_{ar}), 145.8 (C_{ar}), 156.3 (Im-C^2), 192.1 (CO), 196.0 (2 CO). IR (KBr) ν_{CO} 2023 (s), 1994 (s), 1931 (s), 1903 (s), 1888 (s) cm^{-1}. ESI-MS ($C_2H_4Cl_2$) *m/z*: calcd for $C_{34}H_{37}N_2O_6Re_2S_2$ ($[M+H]^+$), 1007.1208; found, 1007.1214. Anal. calcd for $C_{34}H_{36}N_2O_6Re_2S_2$ (1005.20): C, 40.62; H, 3.61; N, 2.79; S, 6.38. Found: C, 38.59; H, 3.31; N, 2.54; S, 6.33.

Part 2 - NMR Spectra

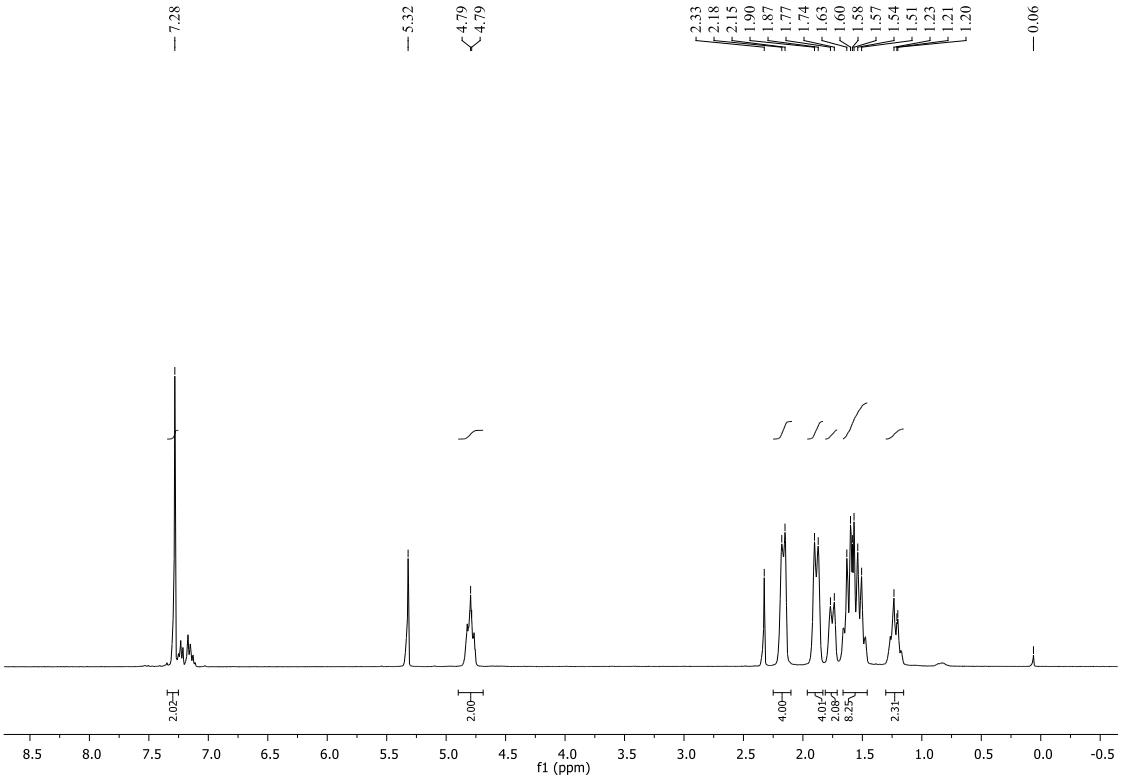

Figure S1. ^{1}H NMR spectrum (400 MHz, CD_2Cl_2, 273 K) of [$ReBr(CO)_3(S_2C{\cdot}ICy)$] (**1**).

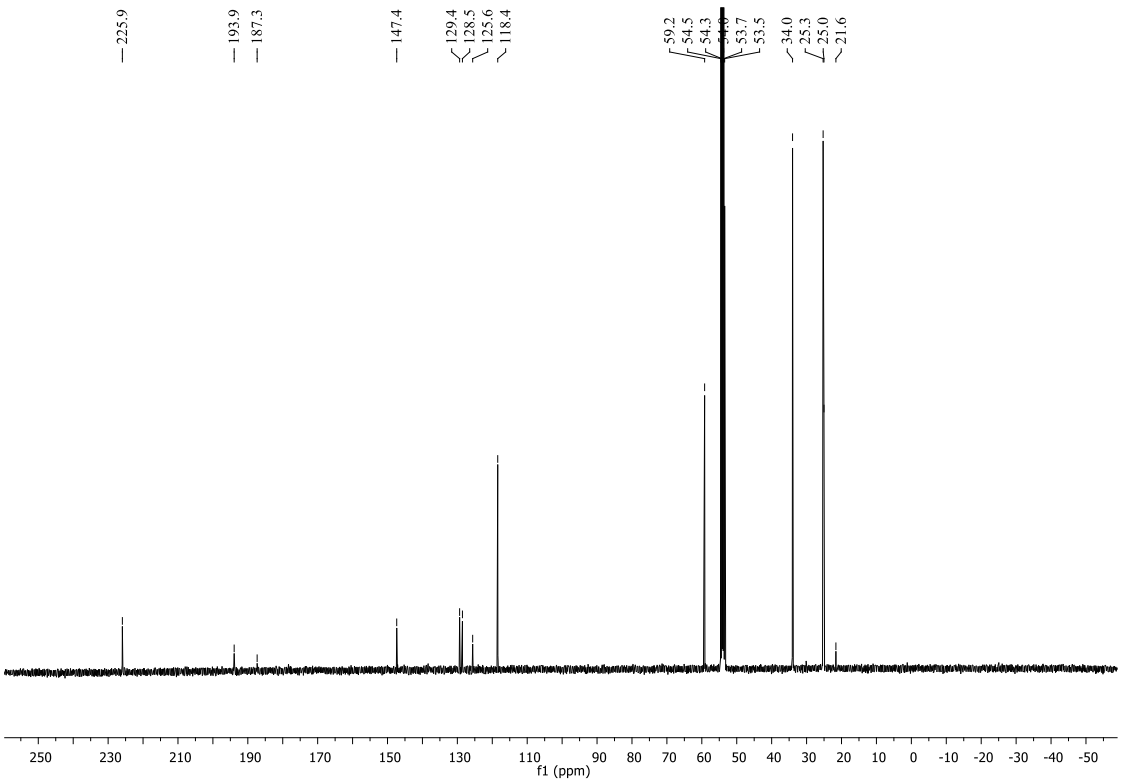

Figure S2. ^{13}C NMR spectrum (100 MHz, CD_2Cl_2, 273 K) of [$ReBr(CO)_3(S_2C{\cdot}ICy)$] (**1**).

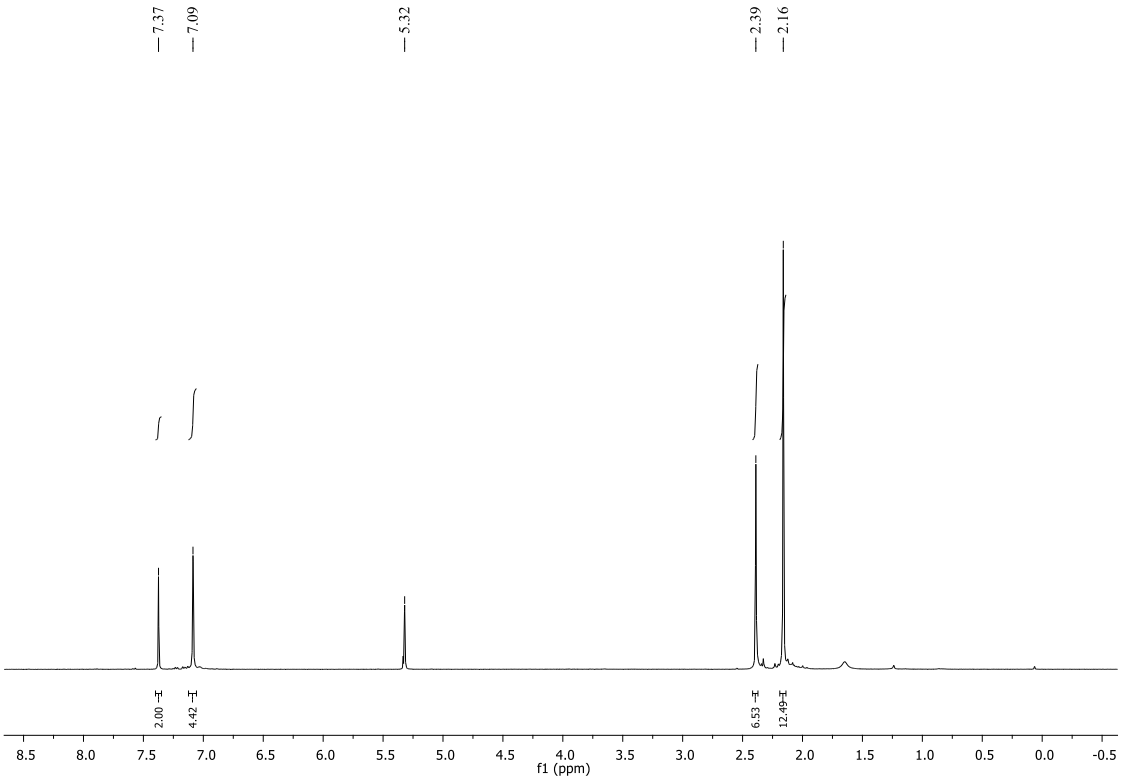

Figure S3. ^{1}H NMR spectrum (400 MHz, CD_2Cl_2, 273 K) of [$ReBr(CO)_3(S_2C{\cdot}IMes)$] (**2**).

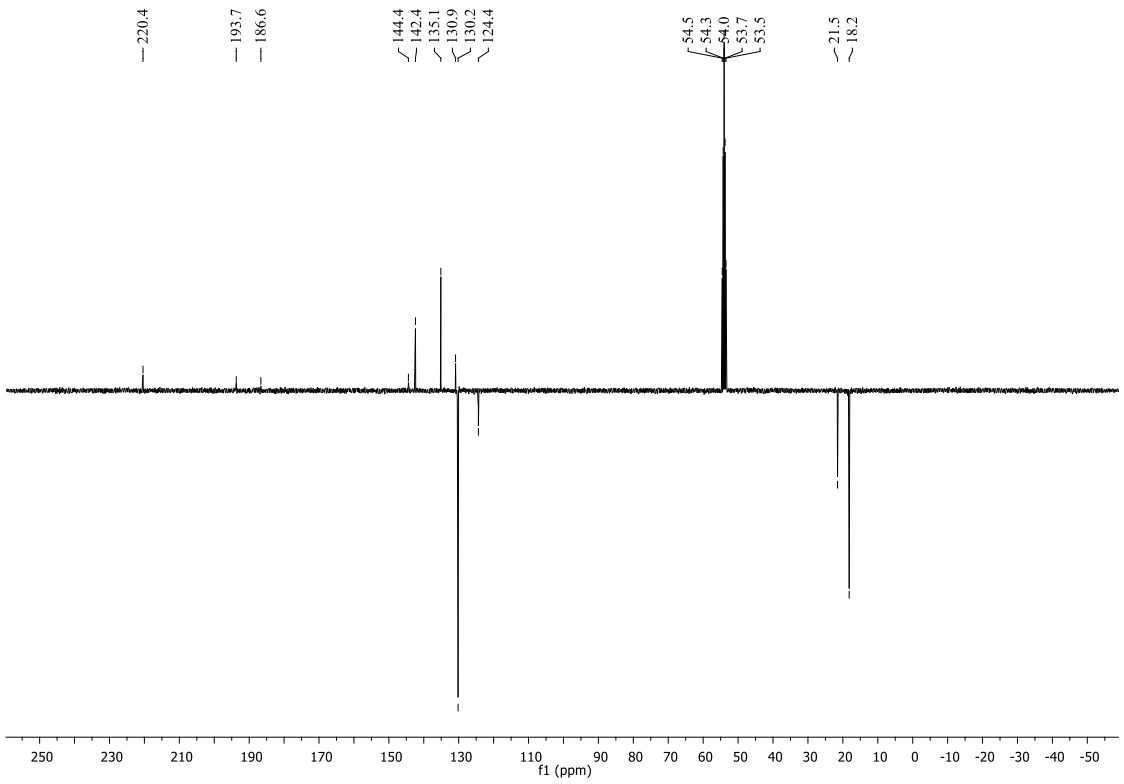

Figure S4. ^{13}C APT NMR spectrum (100 MHz, CD_2Cl_2, 273 K) of [$ReBr(CO)_3(S_2C{\cdot}IMes)$] (**2**).

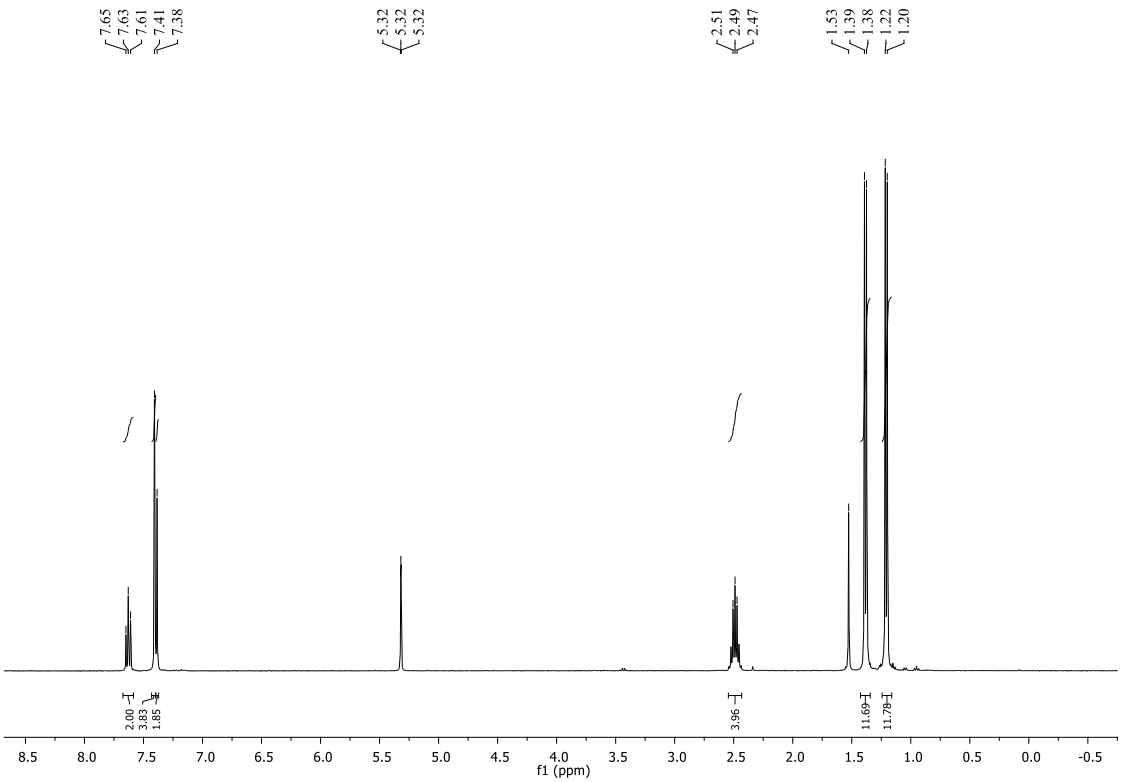

Figure S5. ^{1}H NMR spectrum (400 MHz, CD_2Cl_2, 298 K) of [$ReBr(CO)_3(S_2C{\cdot}IDip)$] (**3**).

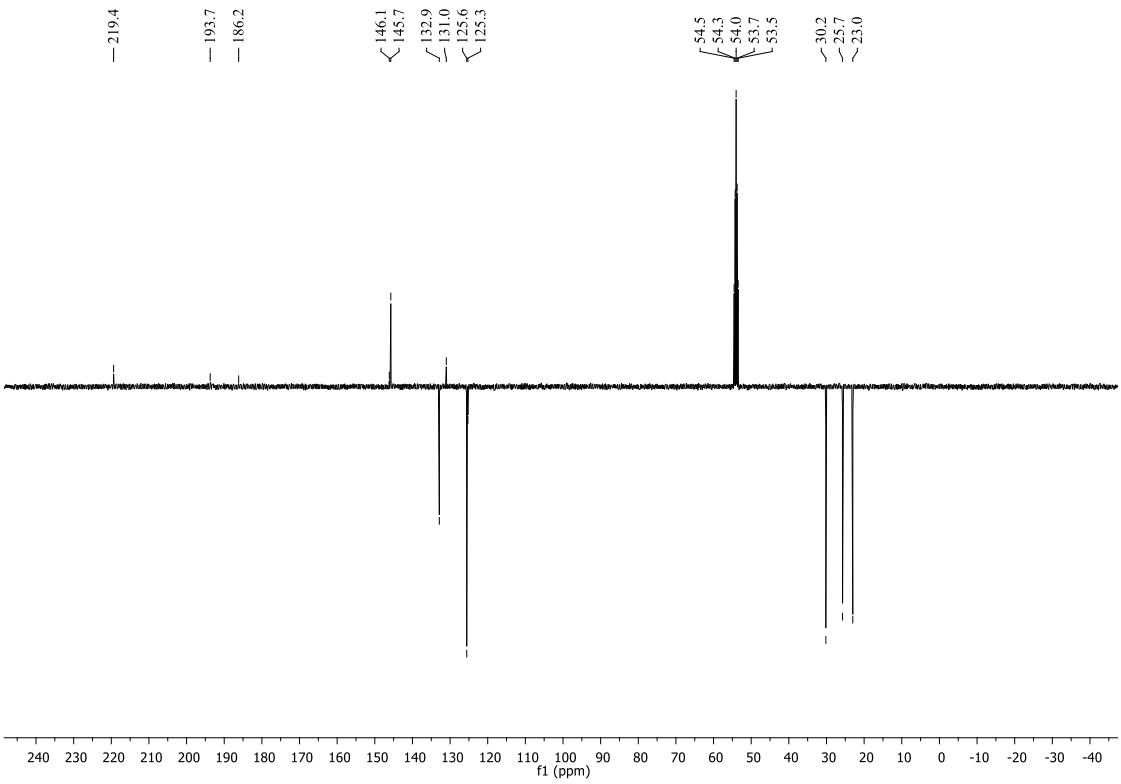

Figure S6. ^{13}C APT NMR spectrum (100 MHz, CD_2Cl_2, 298 K) of [$ReBr(CO)_3(S_2C{\cdot}IDip)$] (**3**).

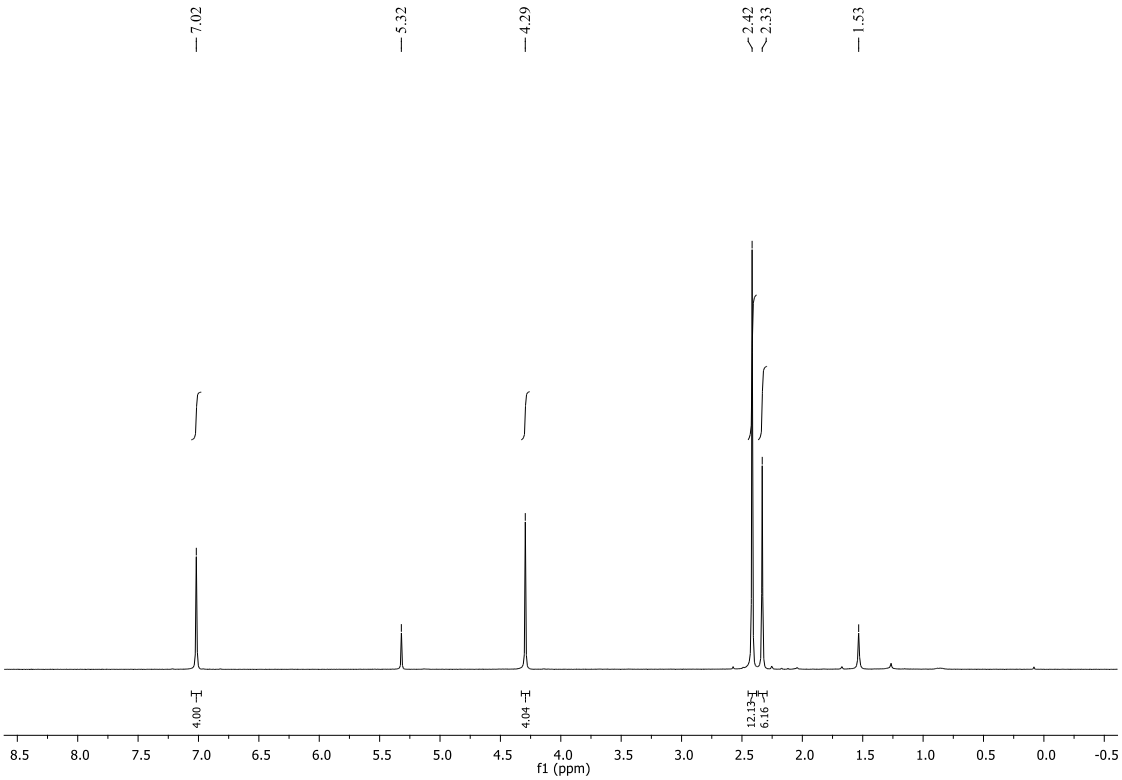

Figure S7. ^{1}H NMR spectrum (400 MHz, CD_2Cl_2, 298 K) of [$ReBr(CO)_3(S_2C{\cdot}SIMes)$] (**4**).

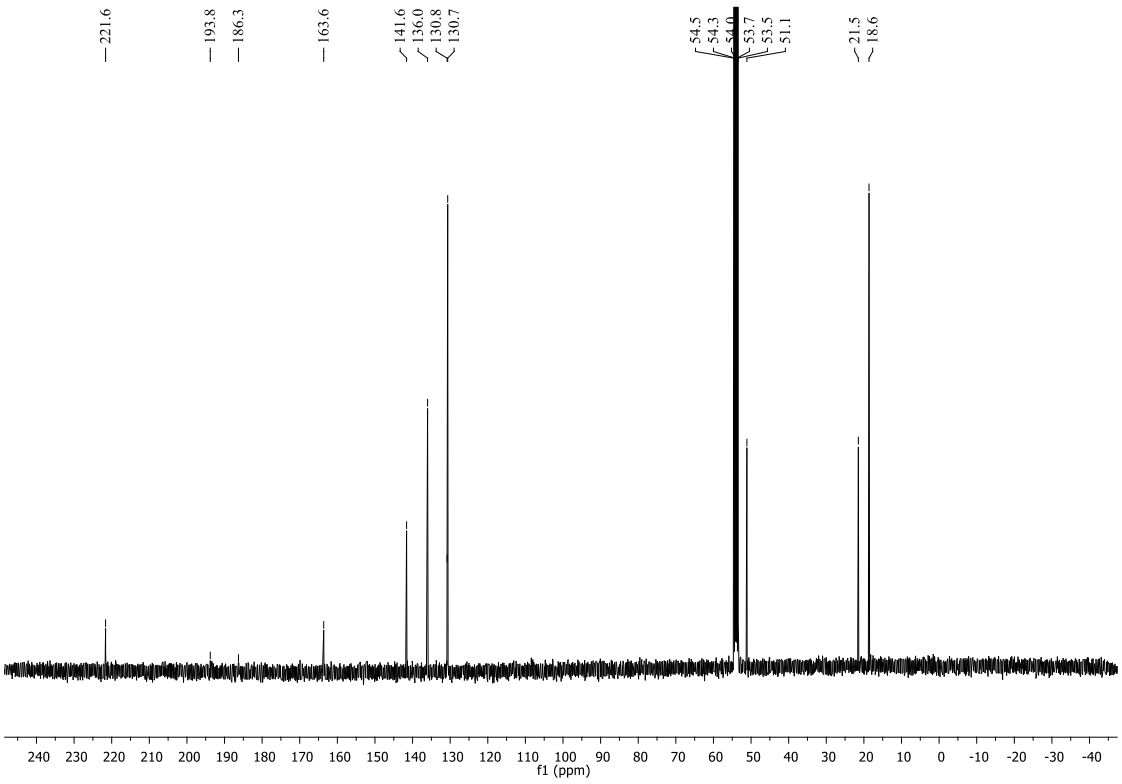

Figure S8. ^{13}C NMR spectrum (100 MHz, CD_2Cl_2, 298 K) of [$ReBr(CO)_3(S_2C{\cdot}SIMes)$] (**4**).

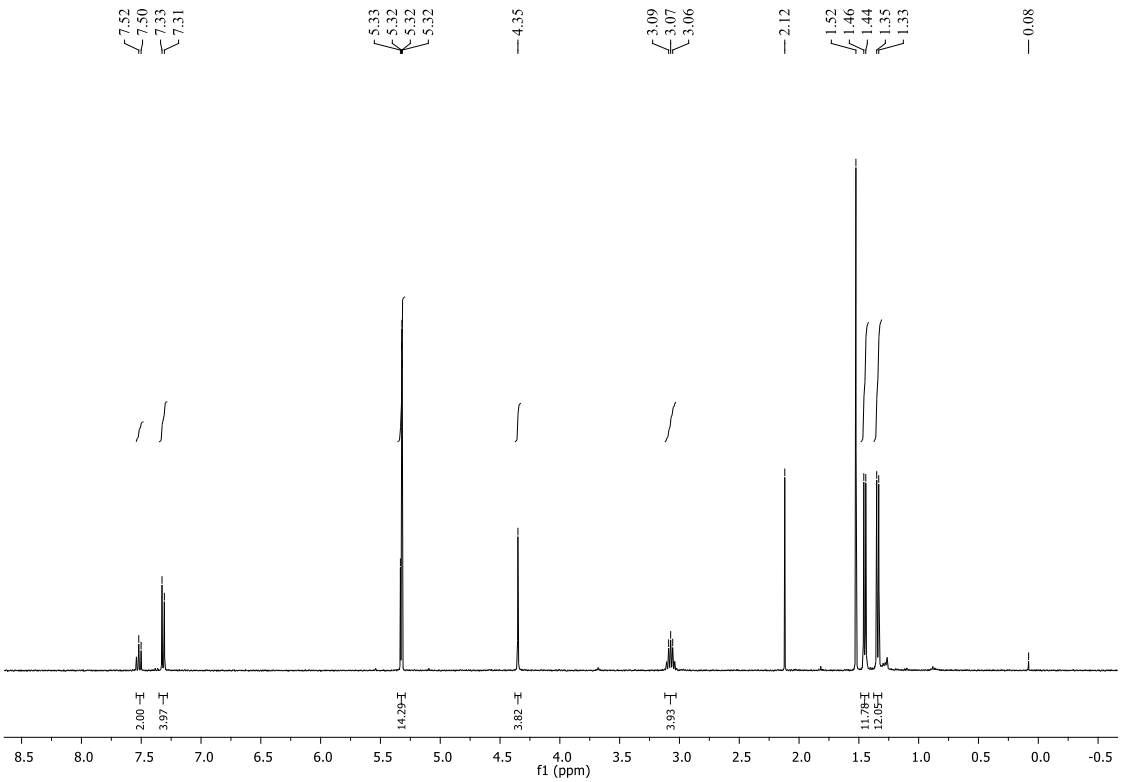

Figure S9. ^{1}H NMR spectrum (400 MHz, CD_2Cl_2, 298 K) of [$ReBr(CO)_3(S_2C{\cdot}SIDip)$] (**5**).

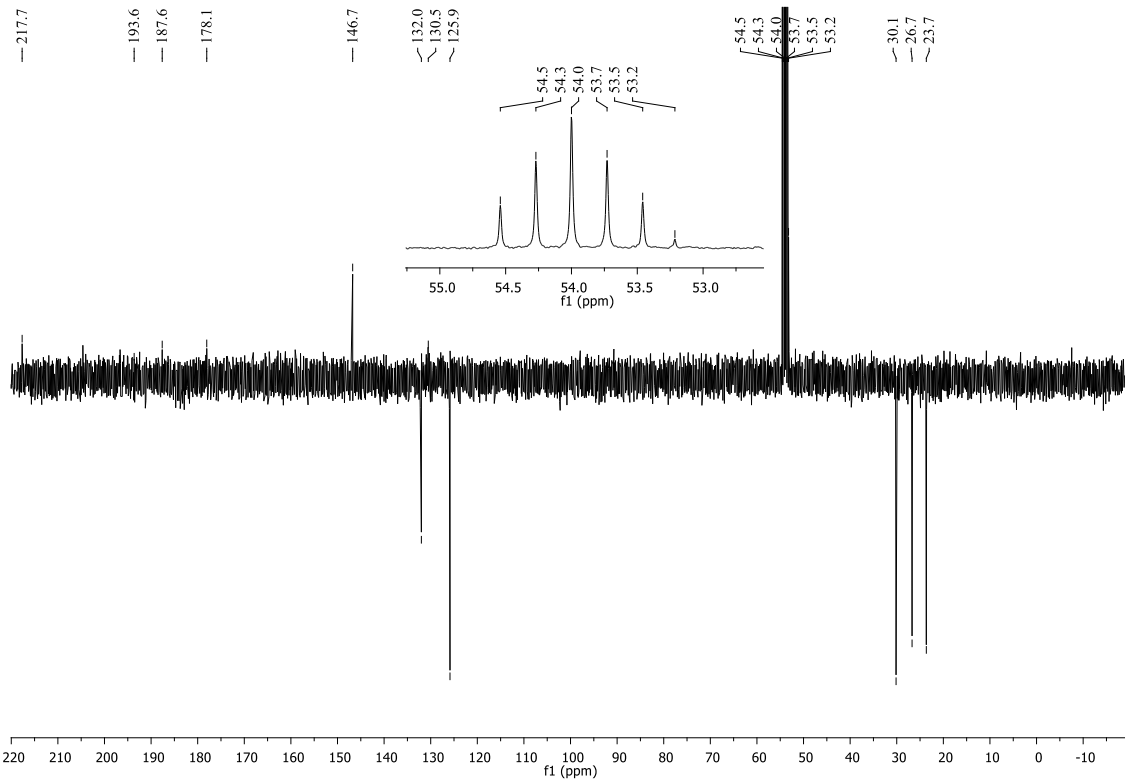

Figure S10. ^{13}C APT NMR spectrum (100 MHz, CD_2Cl_2, 298 K) of [$ReBr(CO)_3(S_2C{\cdot}SIDip)$] (**5**).

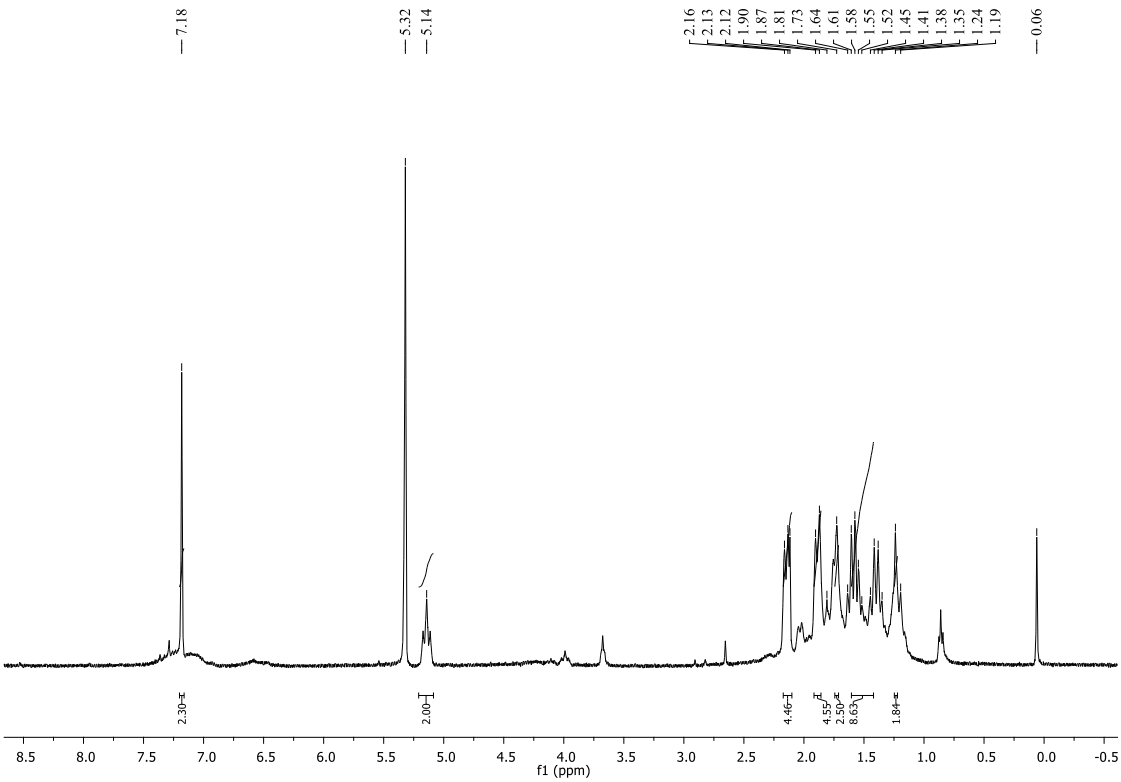

Figure S11. ^{1}H NMR spectrum (400 MHz, CD_2Cl_2, 273 K) of $[Re_2(CO)_8(S_2C{\cdot}ICy)]$ (**6**).

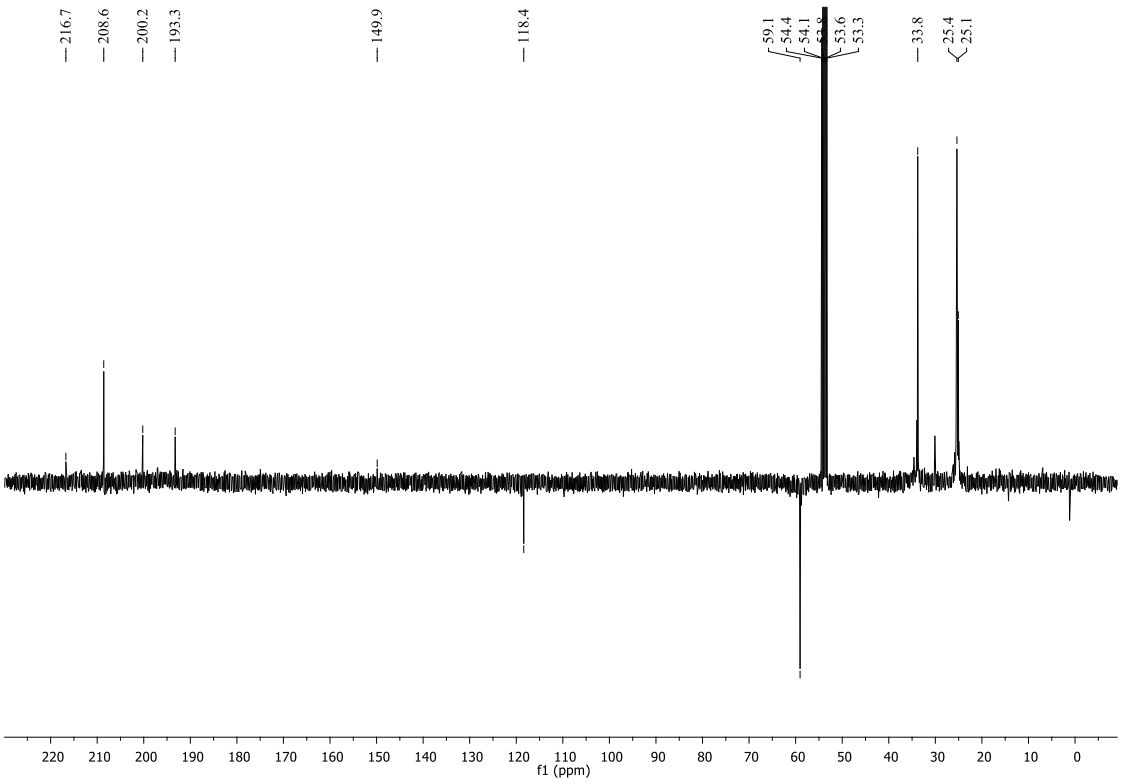

Figure S12. ^{13}C APT NMR spectrum (100 MHz, CD_2Cl_2, 298 K) of $[Re_2(CO)_8(S_2C{\cdot}ICy)]$ (**6**).

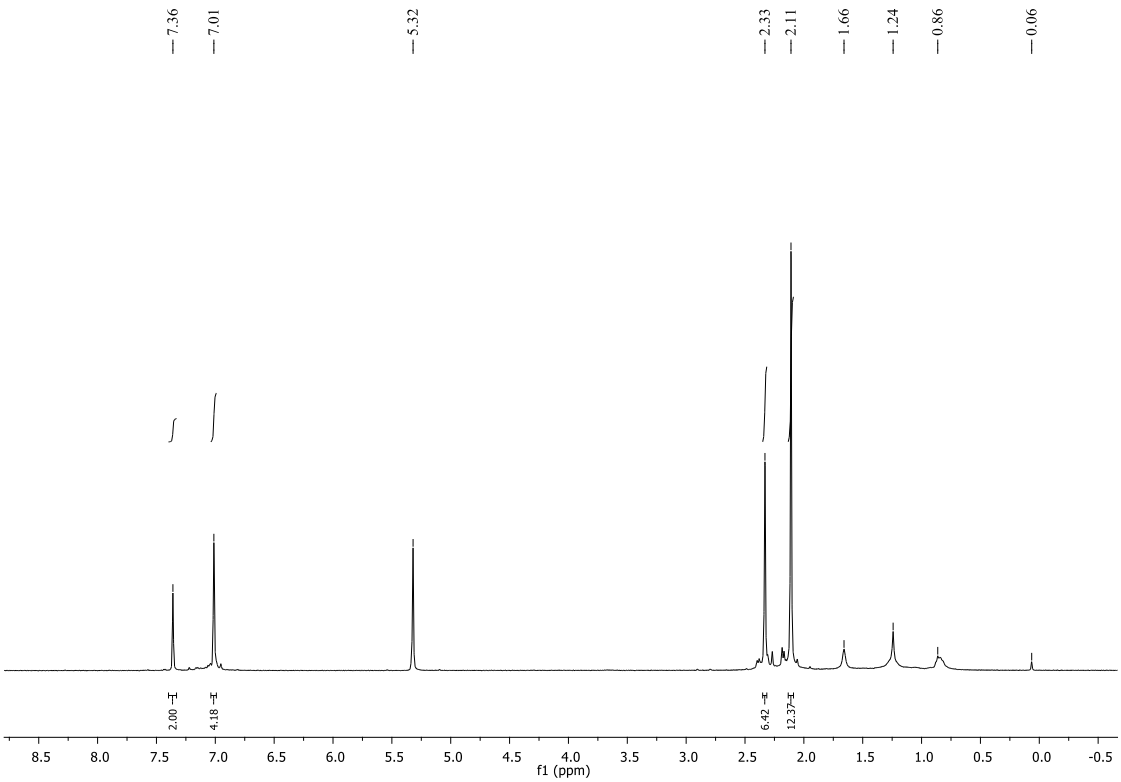

Figure S13. ^{1}H NMR spectrum (400 MHz, CD_2Cl_2, 273 K) of [$Re_2(CO)_8(S_2C{\cdot}IMes)$] (**7**).

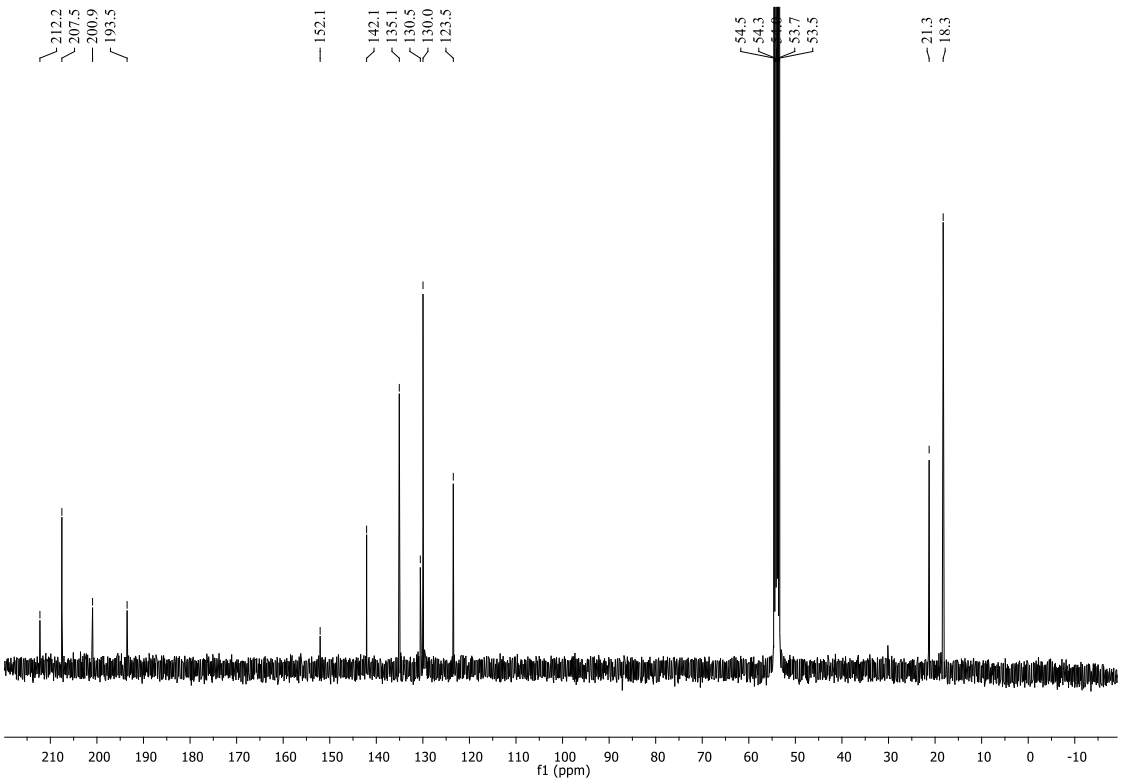

Figure S14. ^{13}C NMR spectrum (100 MHz, CD_2Cl_2, 273 K) of [$Re_2(CO)_8(S_2C{\cdot}IMes)$] (**7**).

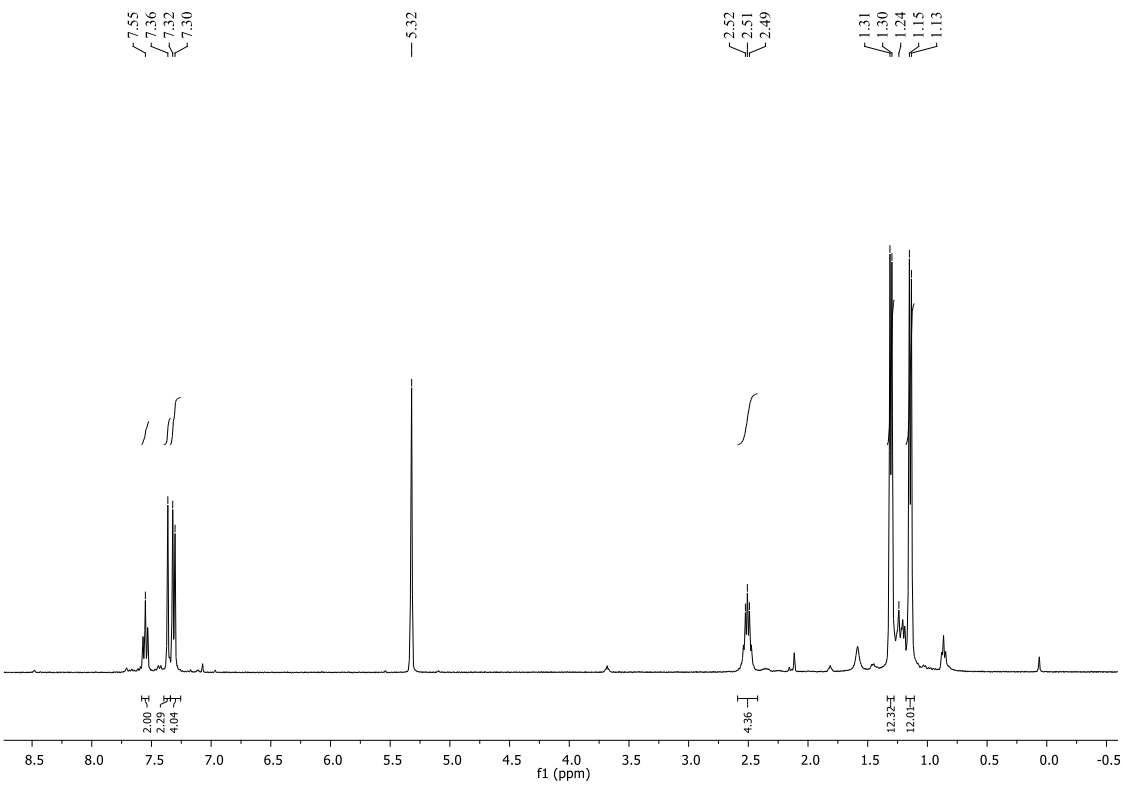

Figure S15. ^{1}H NMR spectrum (400 MHz,CD_2Cl_2, 273 K) of [$Re_2(CO)_8(S_2C{\cdot}IDip)$] (**8**).

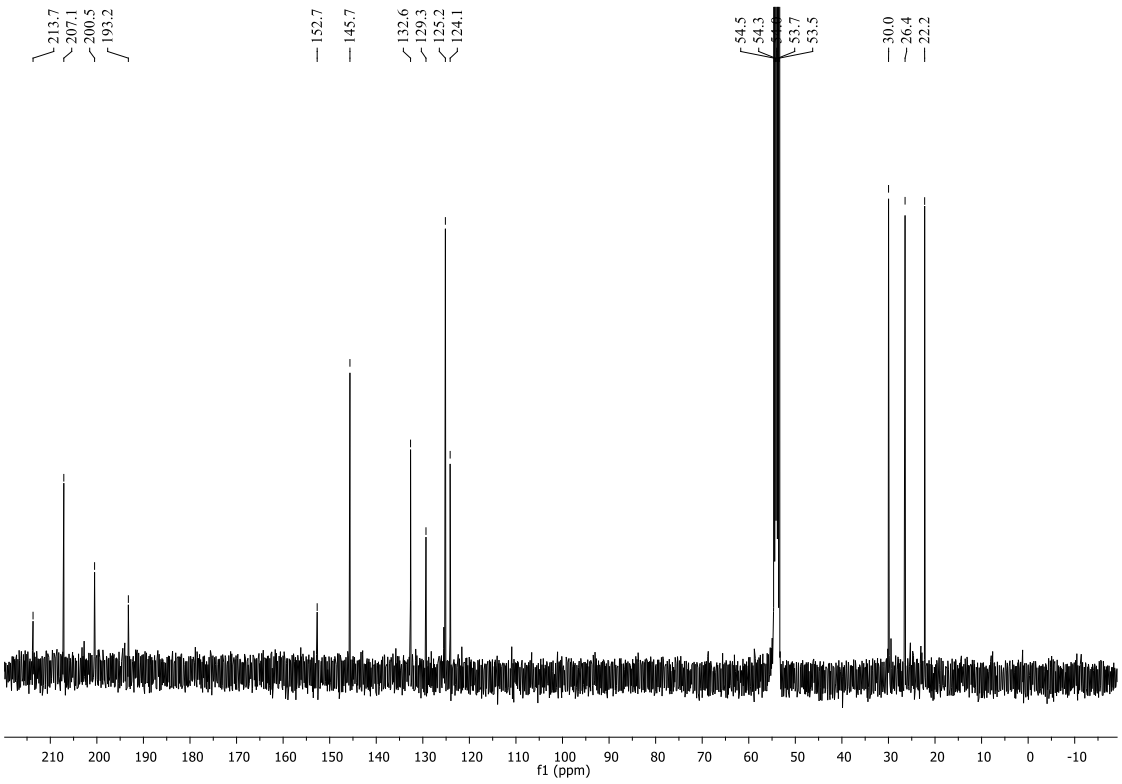

Figure S16. ^{13}C NMR spectrum (100 MHz, CD_2Cl_2, 273 K) of [$Re_2(CO)_8(S_2C{\cdot}IDip)$] (**8**).

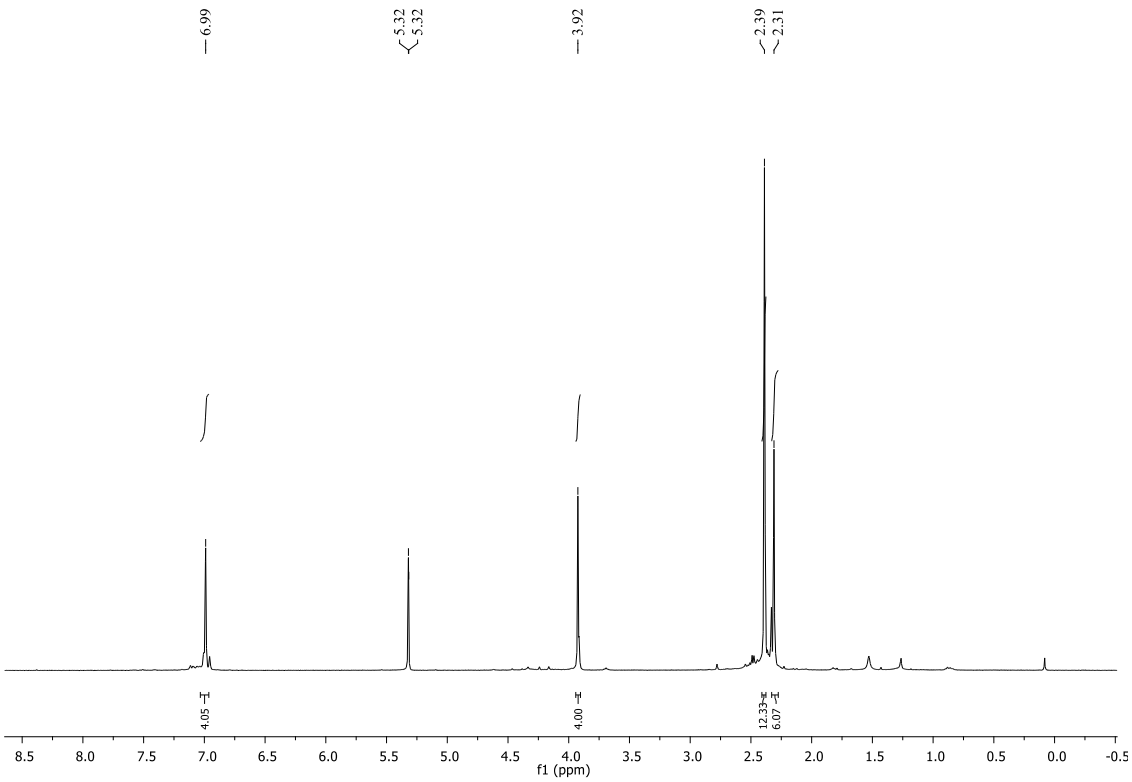

Figure S17. ^{1}H NMR spectrum (400 MHz, CD_2Cl_2, 298 K) of $[Re_2(CO)_6(S_2C{\cdot}SIMes)]$ (**9**).

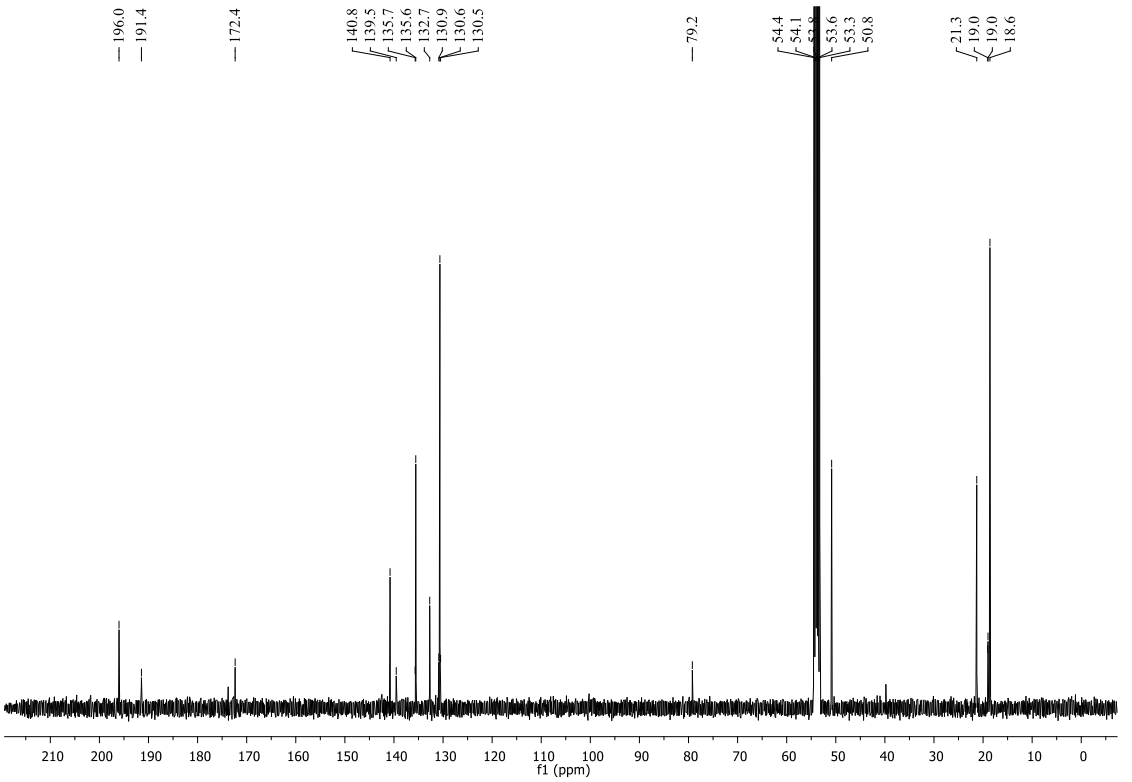

Figure S18. ^{13}C NMR spectrum (100 MHz, CD_2Cl_2, 298 K) of $[Re_2(CO)_6(S_2C{\cdot}SIMes)]$ (**9**).

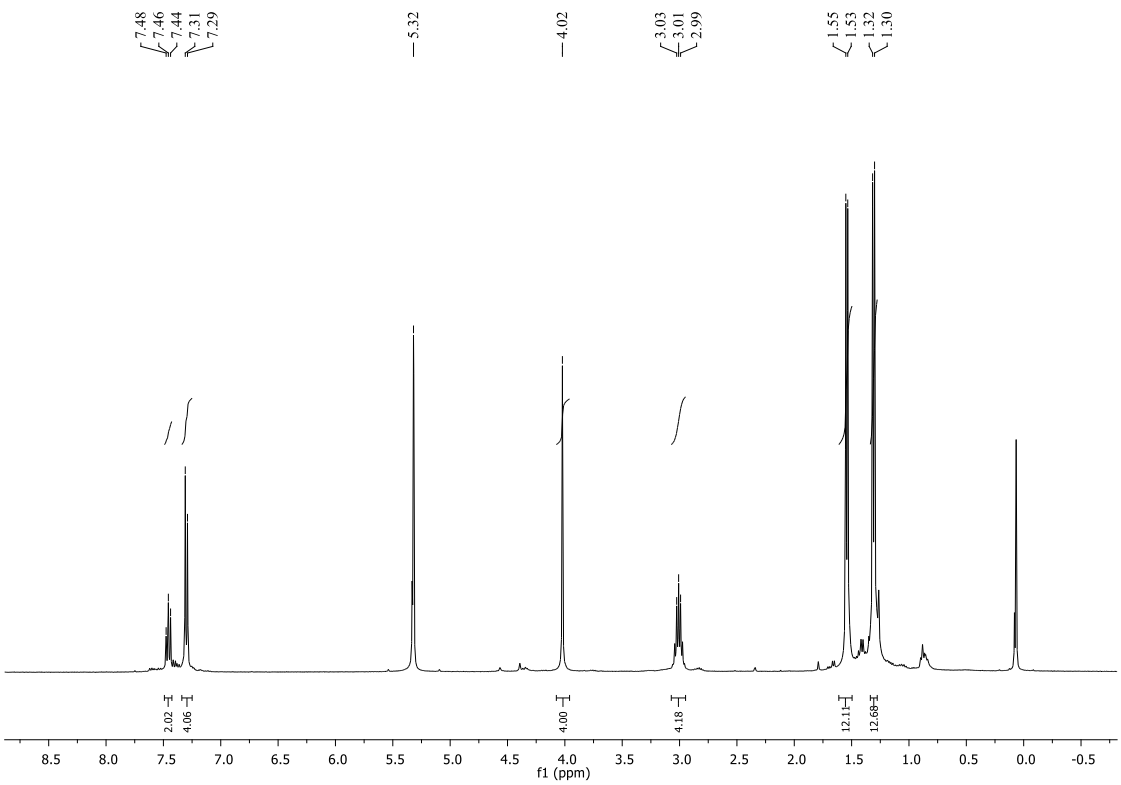

Figure S19. ^{1}H NMR spectrum (400 MHz, CD_2Cl_2, 298 K) of [$Re_2(CO)_6(S_2C{\cdot}SIDip)$] (**10**).

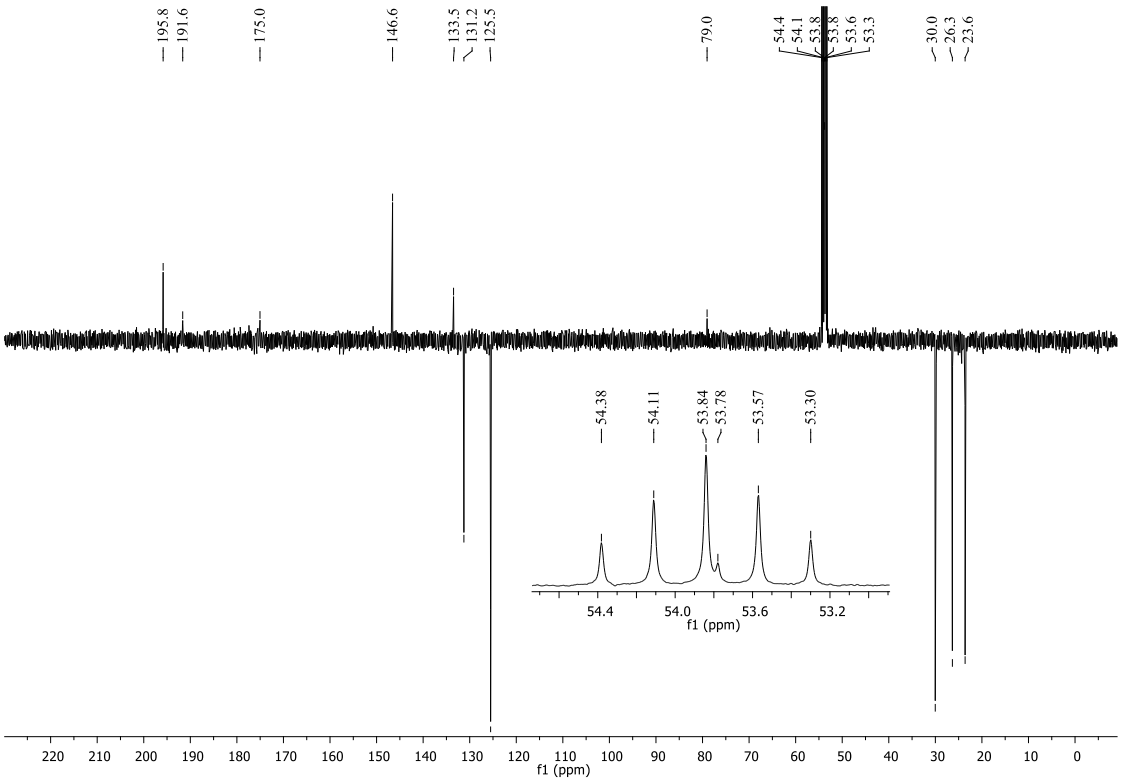

Figure S20. ^{13}C APT NMR spectrum (100 MHz, CD_2Cl_2, 298 K) of [$Re_2(CO)_6(S_2C{\cdot}SIDip)$] (**10**).

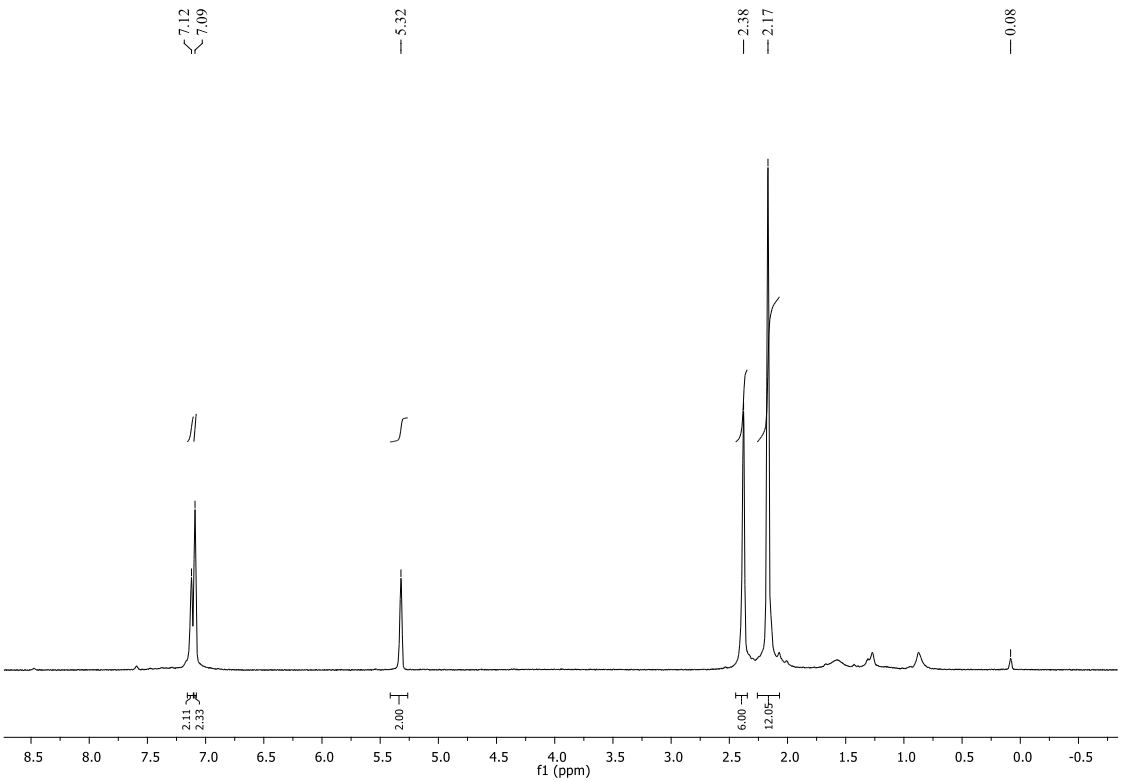

Figure S21. ^{1}H NMR spectrum (400 MHz, CD_2Cl_2, 298 K) of $[Re_2(CO)_6(S_2C{\cdot}IMes)]$ (**11**).

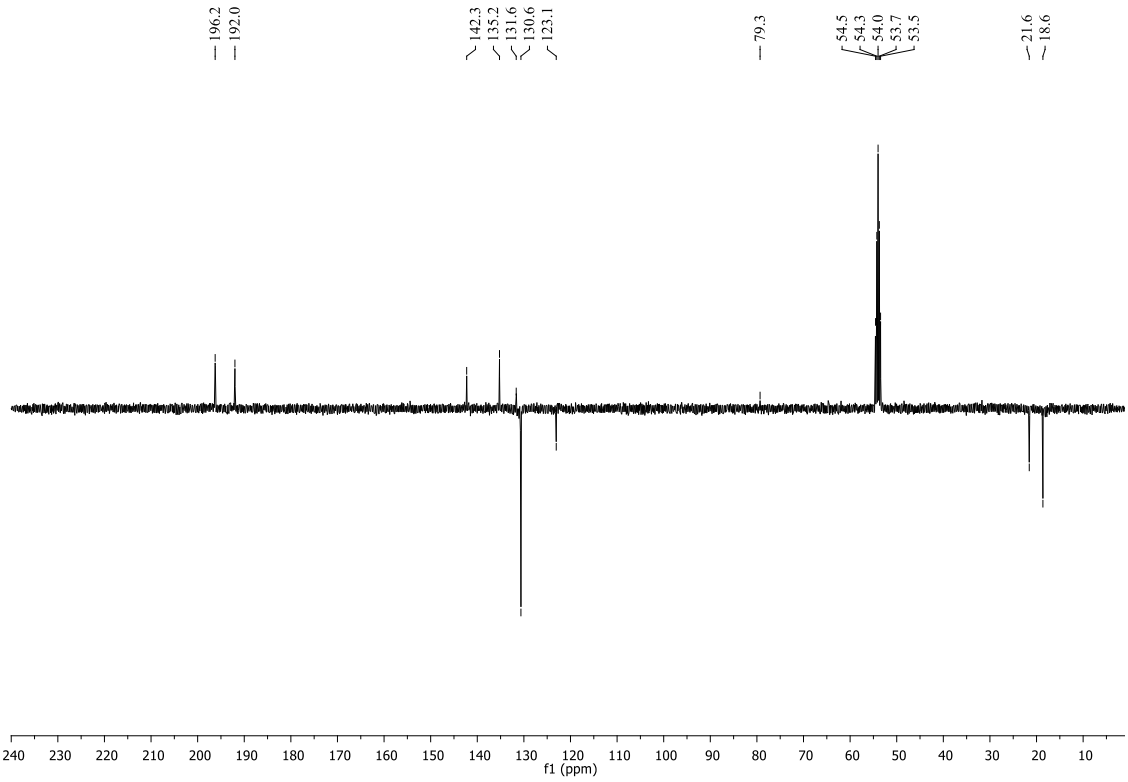

Figure S22. ^{13}C APT NMR spectrum (100 MHz, CD_2Cl_2, 298 K) of $[Re_2(CO)_6(S_2C{\cdot}IMes)]$ (**11**).

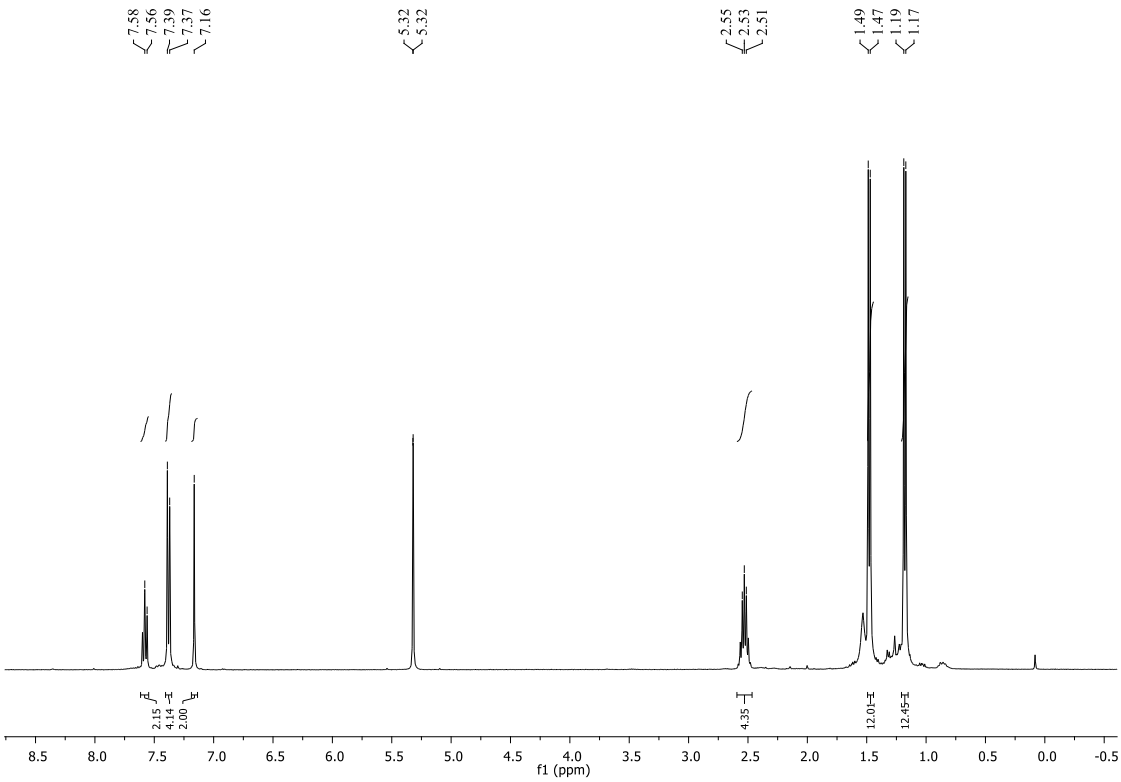

Figure S23. ^{1}H NMR spectrum (400 MHz, CD_2Cl_2, 298 K) of $[Re_2(CO)_6(S_2C{\cdot}IDip)]$ (**12**).

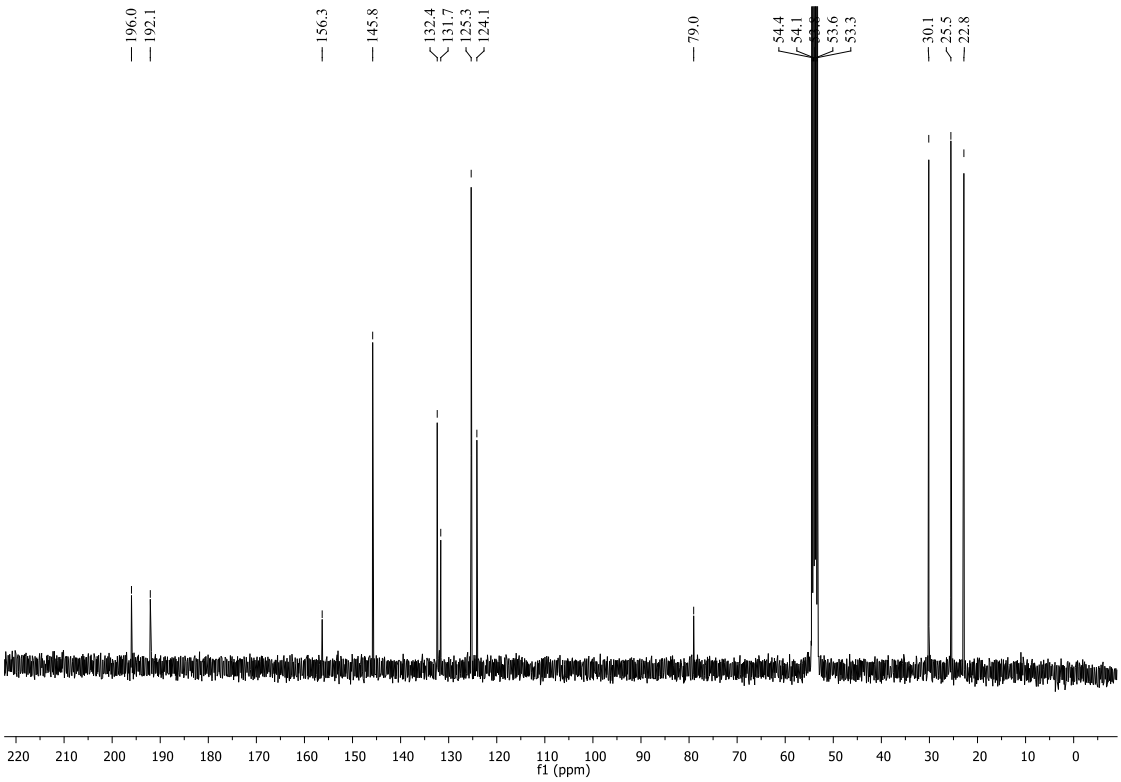

Figure S24. ^{13}C NMR spectrum (100 MHz, CD_2Cl_2, 298 K) of $[Re_2(CO)_6(S_2C{\cdot}IDip)]$ (**12**).

Part 3 - X-Ray Crystallography

1. General Information

X-Ray diffraction analyses were carried out on a Bruker APPEX II diffractometer using Mo-Kα radiation ($\lambda = 0.71073$ Å) from a fine focus sealed tube source at 100 K. Computing data and reduction was made with the APPEX II software.[2] No instrument or crystal instabilities were observed during data collection. Absorption corrections based on the multiscan method were applied.[3] All the structures were solved with DIRDIF2008.[4] They were refined by full-matrix, least-squares based on F^2 using SHELXL.[5] An empirical absorption correction was applied using SADABS.[6] All non-hydrogen atoms were anisotropically refined and the hydrogen atom positions were calculated and refined using a riding model.

2. Crystal Data for Complexes 1, 3–8, 10–12

CCDC 1501949–1501958 contain the supplementary crystallographic data (excluding structure factors) for the structures reported in this paper. These data can be obtained free of charge from The Cambridge Crystallographic Data Centre via https://summary.ccdc.cam.ac.uk/structure-summary-form or on application to CCDC, 12 Union Road, Cambridge CB2 1EZ, UK [fax.: (internat.) +44–1223/336–033].

$[ReBr(CO)_3(S_2C{\cdot}ICy)]_2{\cdot}CH_2Cl_2$ (1). Red crystals with dimensions 0.30 × 0.23 × 0.17 mm obtained by slow diffusion of *n*-hexane into a CH_2Cl_2 solution at 6 °C. $C_{39}H_{50}Br_2Cl_2N_4O_6Re_2S_4$, M = 1402.19, monoclinic, space group $P2_1/c$, a = 10.7763(3) Å, b = 12.5573(4) Å, c = 19.0092(5) Å, α = 90°, β = 102.469(2)°, γ = 90°, V = 2511.67(13) Å^3, T = 100(2) K, Z = 2, μ (Mo Kα) 6.724 mm^{-1}. Reflections collected/unique = 41108/7668 (R_{int} = 0.057). Final refinement converged with R_1 = 0.0437 and wR_2 = 0.06 for all reflections, GOF = 1.012, max/min residual electron density 1.64/–1.03 e·Å^{-3}.

$[ReBr(CO)_3(S_2C{\cdot}IDip)]_2{\cdot}3\ CH_2Cl_2$ (3). Orange crystals with dimensions 0.29 × 0.18 × 0.07 mm obtained by slow diffusion of *n*-hexane into a CH_2Cl_2 solution at 6 °C. $C_{31}H_{36}BrN_2O_3ReS_2$, 1.4($CH_2Cl_2$), M = 933.74, monoclinic, space group $P2_1/n$, a = 11.6006(5) Å, b = 18.0132(7) Å, c = 17.6665(8) Å, α = 90°, β = 91.394(3)°, γ = 90°, V = 2642.5(5) Å^3, T = 100(2) K, Z = 4, μ (Mo Kα) 4.725 mm^{-1}. Reflections collected/unique = 49318 /11324 (R_{int} = 0.035). Final refinement converged with R_1 = 0.0324 and wR_2 = 0.0516 for all reflections, GOF = 1.033, max/min residual electron density 1.29/–0.88 e·Å^{-3}.

[ReBr(CO)$_3$(S$_2$C·SIMes)] (4). Orange crystals with dimensions 0.15 × 0.12 × 0.02 mm obtained by slow diffusion of diethylether into a CH_2Cl_2 solution at 6 °C. $C_{25}H_{26}BrN_2O_3ReS_2$, M = 732.71, monoclinic, space group $P2_1/c$, a = 16.1021(16) Å, b = 10.4186(11) Å, c = 16.2204(18) Å, α = 90°, β = 103.813(4)°, γ = 90°, V = 2642.5(5) Å^3, T = 100(2) K, Z = 4, μ (Mo Kα) 6.298 mm^{-1}. Reflections collected/unique = 26757/4835 (R_{int} = 0.142). Final refinement converged with R_1 = 0.1113 and wR_2 = 0.1216 for all reflections, GOF = 1.015, max/min residual electron density 1.83/–1.74 e·Å^{-3}.

[ReBr(CO)$_3$(S$_2$C·SIDip)]$_2$·3 CH$_2$Cl$_2$ (5). Purple crystals with dimensions 0.29 × 0.18 × 0.07 mm obtained by slow diffusion of toluene into a CH_2Cl_2 solution at 6 °C. $2(C_{31}H_{38}BrN_2O_3ReS_2),3(CH_2Cl_2)$, M = 1888.51, monoclinic, space group $P2_1/n$, a = 11.6384(4) Å, b = 17.8256(7) Å, c = 17.9214(7) Å, α = 90°, β = 91.602(2)°, γ = 90°, V = 3716.5(2) Å^3, T = 100(2) K, Z = 2, μ (Mo Kα) 4.707 mm^{-1}. Reflections collected/unique = 49335/9224 (R_{int} = 0.065). Final refinement converged with R_1 = 0.0461 and wR_2 = 0.0629 for all reflections, GOF = 1.038, max/min residual electron density 0.96/–0.90 e·Å^{-3}.

[Re$_2$(CO)$_8$(S$_2$C·ICy)] (6). Orange crystals with dimensions 0.43 × 0.20 × 0.14 mm obtained by slow diffusion of *n*-hexane into a CH_2Cl_2 solution at –20 °C. $C_{24}H_{24}N_2O_8Re_2S_2$, M = 904.99, trigonal, space group $P3_121$, a = 12.578(2) Å, b = 12.578(2) Å, c = 15.381(4) Å, α = 90°, β = 90°, γ = 120°, V = 2107.5(10) Å^3, T = 100(2) K, Z = 3, μ (Mo Kα) 8.805 mm^{-1}. Reflections collected/unique = 100588/4903 (R_{int} = 0.0689). Final refinement converged with R_1 = 0.0257 and wR_2 = 0.0439 for all reflections, GOF = 1.103, max/min residual electron density 2.23/–1.49 e·Å^{-3}.

[Re$_2$(CO)$_8$(S$_2$C·IMes)] (7). Reddish-brown crystals with dimensions 0.35 × 0.16 × 0.03 mm obtained by slow diffusion of *n*-hexane into a CH_2Cl_2 solution at –20 °C. $C_{30}H_{24}N_2O_8Re_2S_2$, M = 977.03, monoclinic, space group $P2/c$, a = 18.1803(9) Å, b = 12.7701(5) Å, c = 15.0641(8) Å, α = 90°, β = 114.425(3)°, γ = 90°, V = 3184.3(3) Å^3, T = 100(2) K, Z = 4, μ (Mo Kα) 7.778 mm^{-1}. Reflections collected/unique = 69169/9710 (R_{int} = 0.058). Final refinement converged with R_1 = 0.0313 and wR_2 = 0.0658 for all reflections, GOF = 1.082, max/min residual electron density 2.65/–2.39 e·Å^{-3}.

[Re$_2$(CO)$_8$(S$_2$C·IDip)]·*n*-C$_6$H$_{14}$ (8). Brown crystals with dimensions 0.42 × 0.15 × 0.08 mm obtained by slow diffusion of *n*-hexane into a CH_2Cl_2 solution at –20 °C. $C_{36}H_{36}N_2O_8Re_2S_2,C_6H_{14}$, M = 1147.36, monoclinic, space group $I2/a$, a = 18.344(2) Å, b = 17.695(2) Å, c = 28.817(4) Å, α = 90°, β = 101.112(2)°, γ = 90°, V = 9179(2) Å^3, T = 100(2) K, Z = 8, μ (Mo Kα) 5.41 mm^{-1}.

Reflections collected/unique = 59453/9388 (R_{int} = 0.068). Final refinement converged with R_1 = 0.0441 and wR_2 = 0.0663 for all reflections, GOF = 1.036, max/min residual electron density 0.87/–0.78 e·Å^{-3}.

[$Re_2(CO)_6(S_2C{\cdot}SIDip)]_2{\cdot}CH_2Cl_2$ (10). Yellow-brown crystals with dimensions 0.13 × 0.12 × 0.08 mm obtained by slow diffusion of *n*-hexane into a CH_2Cl_2 solution at –20 °C. $2(C_{34}H_{38}N_2O_6Re_2S_2),CH_2Cl_2'$, M = 2099.33, orthorhombic, space group Aba2, a = 38.243(4) Å, b = 11.6015(11) Å, c = 16.5828(19) Å, α = 90°, β = 90°, γ = 90º, V = 7357.4(13) Å^3, T = 100(2) K, Z = 4, μ (Mo Kα) 6.806 mm^{-1}. Reflections collected/unique = 28772 / 8332 (R_{int} = 0.0783). Final refinement converged with R_1 = 0.0695 and wR_2 = 0.1013 for all reflections, GOF = 0.997, max/min residual electron density 1.61/–1.96 e·Å^{-3}.

[$Re_2(CO)_6(S_2C{\cdot}IMes)]_2{\cdot}CH_2Cl_2$ (11). Orange-brown crystals with dimensions 0.35 × 0.23 × 0.18 mm obtained by slow diffusion of *n*-hexane into a CH_2Cl_2 solution at –20 °C. $2(C_{28}H_{24}N_2O_6Re_2S_2),CH_2Cl_2$, M = 1926.99, monoclinic, space group $P2_1/n$, a = 14.1331(4) Å, b = 11.0904(3) Å, c = 20.4981(5) Å, α = 90°, β = 104.559(2)°, γ = 90º, V = 3109.74(15) Å^3, T = 100(2) K, Z = 2, μ (Mo Kα) 8.042 mm^{-1}. Reflections collected/unique = 56585 / 6603 (R_{int} = 0.0586). Final refinement converged with R_1 = 0.0273 and wR_2 = 0.0437 for all reflections, GOF = 1.036, max/min residual electron density 0.91/–0.8 e·Å^{-3}.

[$Re_2(CO)_6(S_2C{\cdot}IDip)]_2{\cdot}CH_2Cl_2$ (12). Yellow-brown crystals with dimensions 0.07 × 0.06 × 0.05 mm obtained by slow diffusion of *n*-hexane into a CH_2Cl_2 solution at –20 °C. $2(C_{34}H_{36}N_2O_6Re_2S_2)$, CH_2Cl_2, M = 2095.30, orthorhombic, space group Aba2, a = 37.853(3) Å, b = 11.6230(9) Å, c = 16.6584(12) Å, α = 90°, β = 90°, γ = 90º, V = 7329.1(10) Å^3, T = 100(2) K, Z = 4, μ (Mo Kα) 6.833 mm^{-1}. Reflections collected/unique = 56012/56012 (R_{int} = 0.0887). Final refinement converged with R_1 = 0.1548 and wR_2 = 0.2116 for all reflections, GOF = 1.004, max/min residual electron density 2.82/–2.68 e·Å^{-3}.

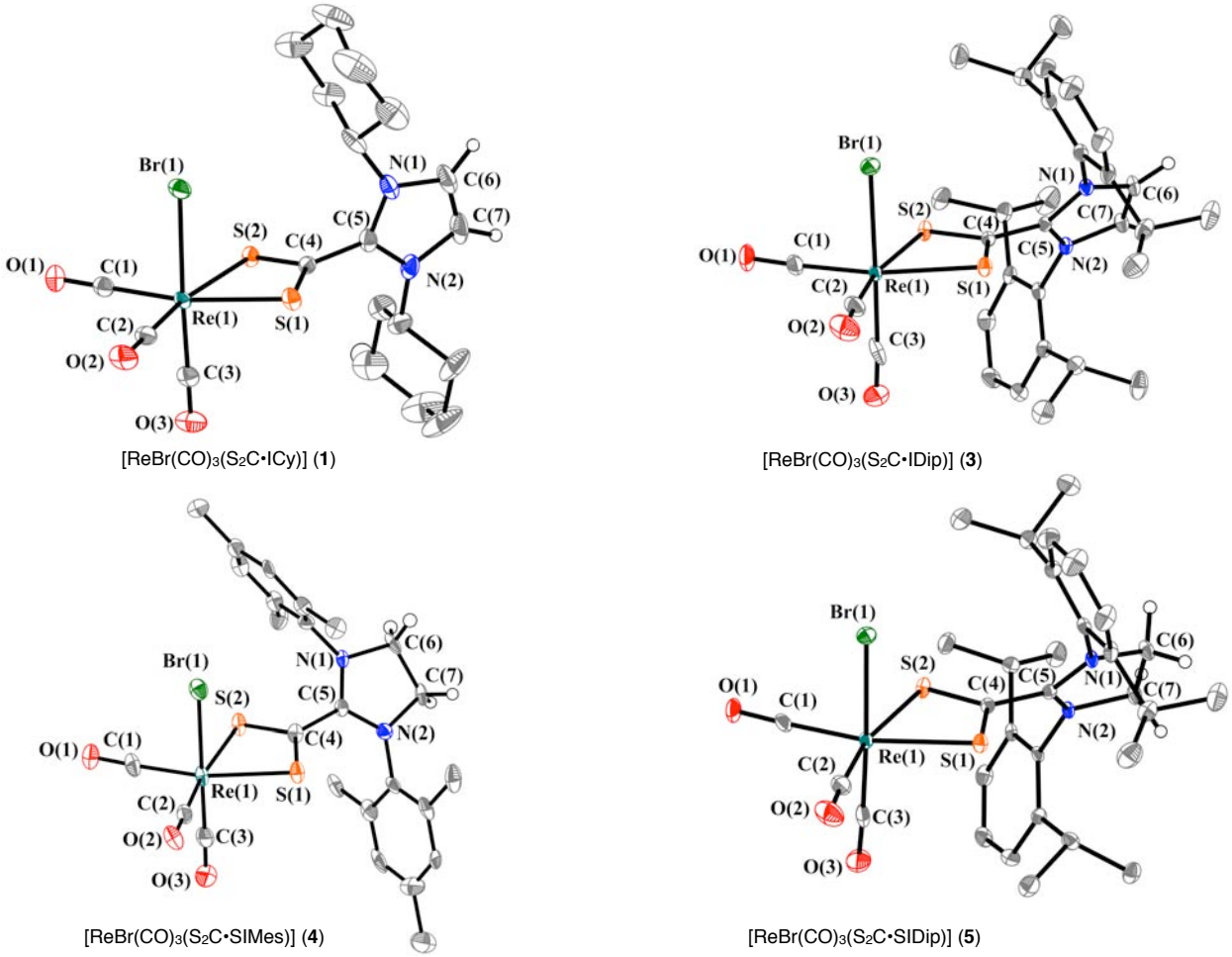

Figure S25. ORTEP representations of [ReBr(CO)$_3$(S$_2$C·ICy)] (**1**), [ReBr(CO)$_3$(S$_2$C·IDip)] (**3**), [ReBr(CO)$_3$(S$_2$C·SIMes)] (**4**), and [ReBr(CO)$_3$(S$_2$C·SIDip)] (**5**) (ellipsoids drawn at the 50% probability level). Co-crystallized solvent molecules and hydrogen atoms were omitted, except those directly bonded to the heterocyclic ring in order to emphasize the presence or the absence of a double bond.

Table S1. Selected Bond Distances (Å) and Angles (deg) Derived from the Molecular Structures of Complexes **1**, **3**, **4**, and **5**[a]

Complex	**1**	**3**	**4**	**5**
Re–C(1)	1.912(4)	1.908(3)	1.901(12)	1.904(4)
Re–C(2)	1.918(3)	1.926(3)	1.918(13)	1.929(4)
Re–C(3)	1.893(4)	1.947(4)	1.863(13)	1.914(4)
Re–S(1)	2.5099(8)	2.5057(7)	2.527(3)	2.5072(8)
Re–S(2)	2.5070(8)	2.5062(3)	2.480(3)	2.5172(8)
Re–Br(1)	2.6241(4)	2.6192(3)	2.6338(13)	2.6266(3)
C(4)–S(1)	1.671(3)	1.672(3)	1.668(10)	1.675(3)
C(4)–S(2)	1.666(3)	1.676(3)	1.688(11)	1.673(3)
C(4)–C(5)	1.477(4)	1.465(4)	1.497(14)	1.484(4)
N(1)–C(5)	1.341(4)	1.342(3)	1.312(12)	1.317(4)
N(2)–C(5)	1.324(5)	1.348(3)	1.319(12)	1.325(4)
C(6)–C(7)	1.331(6)	1.349(4)	1.547(14)	1.531(4)
C(1)–Re(1)–C(2)	89.81(5)	93.25(15)	91.9(5)	93.37(16)
C(1)–Re(1)–C(3)	90.87(15)	90.17(14)	93.6(5)	89.64(14)
C(2)–Re(1)–C(3)	91.79(14)	88.67(10)	87.1 (5)	88.90(16)
C(1)–Re(1)–S(1)	169.35(10)	168.21(11)	166.5(4)	168.12(11)
C(1)–Re(1)–S(2)	101.82(10)	99.46(11)	97.5(4)	99.81(12)
C(1)–Re(1)–Br(1)	88.83(10)	88.35(10)	87.0(4)	87.98(10)
S(1)–Re(1)–S(2)	69.55(3)	69.68(2)	69.71(9)	69.66(3)
S(1)–C(4)–S(2)	118.06(18)	117.56(16)	117.0(6)	117.99(18)
N(1)–C(5)–C(4)–S(1)	–80.2(4)	–56.5(3)	–127.9(10)	–57.9(4)
N(2)–C(5)–C(4)–S(1)	102.6(4)	121.6(2)	50.5(14)	125.1(3)

[a]See Figure S25 for atom labeling.

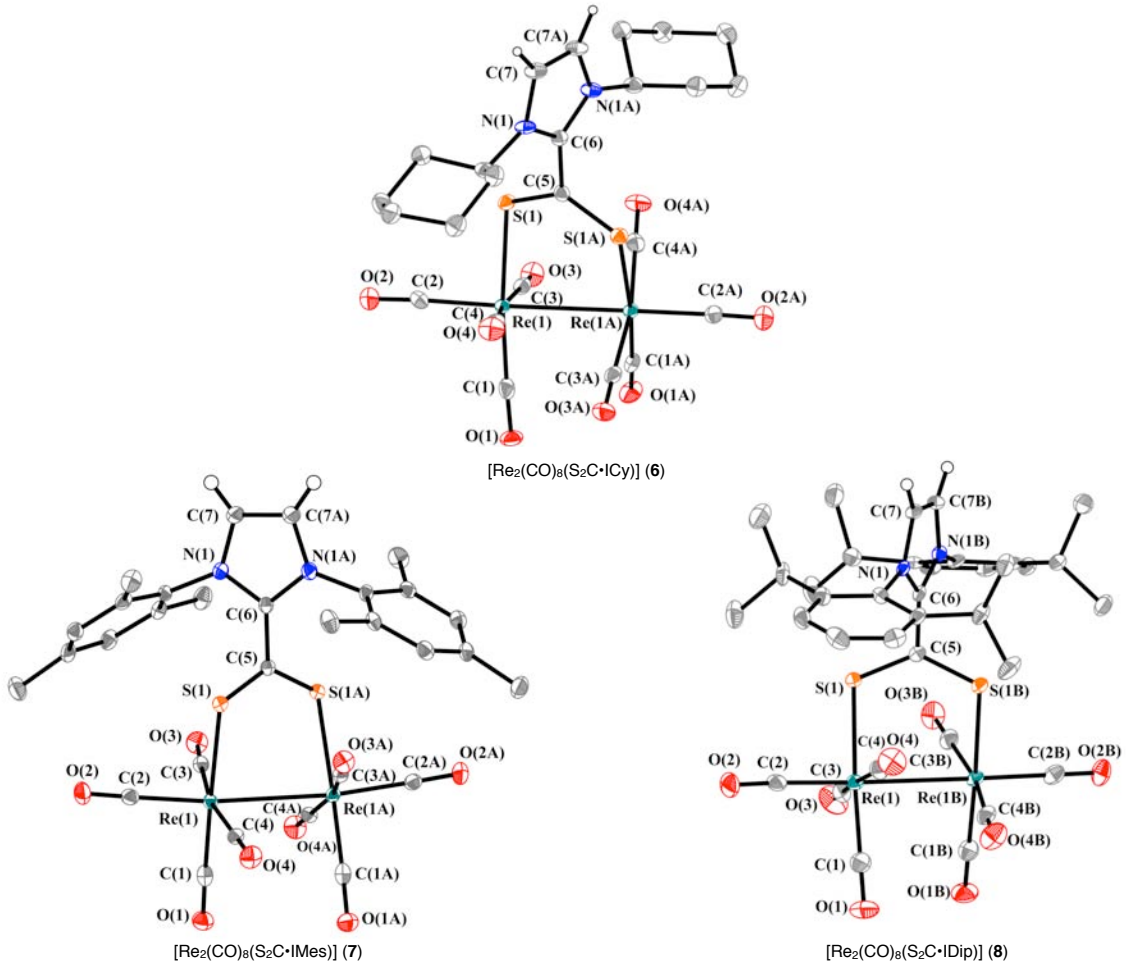

Figure S26. ORTEP representations of $[Re_2(CO)_8(S_2C{\cdot}ICy)]$ (**6**), $[Re_2(CO)_8(S_2C{\cdot}IMes)]$ (**7**), and $[Re(CO)_8(S_2C{\cdot}IDip)]$ (**8**) (ellipsoids drawn at the 50% probability level). Co-crystallized solvent molecules and hydrogen atoms were omitted, except those directly bonded to the heterocyclic ring in order to emphasize the presence of a double bond. Only one of the two molecules present in the asymmetric unit of 7 is depicted.

Table S2. Selected Bond Distances (Å) and Angles (deg) Derived from the Molecular Structures of Complexes **6**–**8**[a]

Complex	**6**	**7_1**	**7_2**	**8**	**8B**
Re(1)–Re(1*)	2.9722(8)	2.9578(4)	2.9661(4)	2.9873(3)	2.9873(3)
Re(1)–C(1)	1.929(5)	1.920(5)	1.921(5)	1.929(5)	1.939(5)
Re(1)–C(2)	1.926(5)	1.938(5)	1.935(5)	1.933(5)	1.915(5)
Re(1)–C(3)	1.993(5)	1.991(5)	1.979(5)	1.993(6)	1.992(5)
Re(1)–C(4)	1.983(5)	1.982(5)	1.982(5)	1.976(5)	1.993(5)
Re(1)–S(1)	2.4586(13)	2.4632(11)	2.4550(11)	2.4493(11)	2.4614(12)
S(1)–C(5)	1.680(3)	1.679(3)	1.682(3)	1.683(5)	1.676(5)
C(5)–C(6)	1.478(9)	1.471(9)	1.465(9)	1.475(5)	1.475(5)
N(1)–C(6)	1.346(6)	1.350(5)	1.344(5)	1.342(3)	1.343(5)
C(7)–C(7*)	1.343(5)	1.369(10)	1.357(12)	1.336(6)	1.336(6)
C(1)–Re(1)–C(2)	95.3(2)	94.3(2)	95.8(2)	91.8 (2)	92.0(2)
C(1)–Re(1)–C(3)	92.6(2)	90.72(19)	92.4(2)	91.0(2)	90.1(2)
C(1)–Re(1)–C(4)	89.7(2)	90.56(19)	91.4(2)	91.5(2)	91.1(2)
C(1)–Re(1)–S(1)	172.06(15)	176.66(14)	176.87(16)	176.60(16)	175.01(15)
C(2)–Re(1)–Re(1*)	177.60(14)	173.83(14)	173.66(16)	176.28(14)	177.46(16)
C(3)–Re(1)–C(4)	170.89(19)	168.9(2)	171.08(19)	168.86(19)	171.9(2)
S(1)–C(5)–S(1*)	131.4(4)	129.6(4)	129.3(4)	130.5(3)	130.5(3)
N(1)–C(6)–C(5)–S(1)	78.8(2)	–57.0(2)	–57.5(3)	72.6(5)	75.0 (5)
C(1)–Re(1)–Re(2)–C(1*)	41.0(3)	–39.1(2)	–34.1(2)	35.5(2)	35.5(2)

[a]See Figure S26 for atom labeling. The star corresponds to the A label for complexes **6** and **7** with half-molecules in their asymmetric unit and to the B label for the other half-molecule in complex **8**.

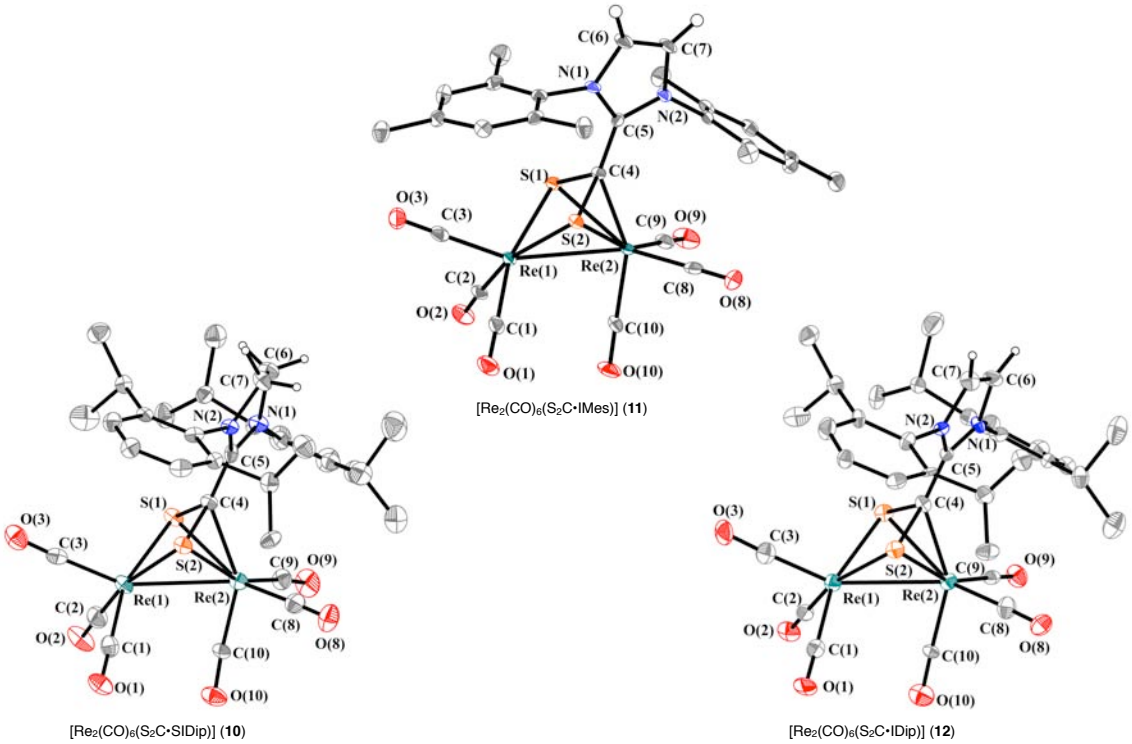

Figure S27. ORTEP representations of $[Re_2(CO)_6(S_2C{\cdot}SIDip)]$ (**10**), $[Re_2(CO)_6(S_2C{\cdot}IMes)]$ (**11**), and $[Re_2(CO)_6(S_2C{\cdot}IDip)]$ (**12**) (ellipsoids drawn at the 50% probability level). Co-crystallized CH_2Cl_2 molecules and hydrogen atoms were omitted, except those directly bonded to the heterocyclic ring in order to emphasize the presence or the absence of a double bond.

Table S3. Selected Bond Distances (Å) and Angles (deg) Derived from the Molecular Structures of Complexes **10–12**[a]

Complex	**10**	**11**	**12**
Re(1)–Re(2)	2.9471(9)	2.9624(2)	2.943(2)
Re(1)–C(1)	1.879(18)	1.926(4)	1.87(4)
Re(1)–C(2)	1.933(16)	1.922(4)	1.94(4)
Re(1)–C(3)	1.889(17)	1.887(4)	1.88(4)
Re(2)–C(8)	1.970(15)	1.919(4)	1.92(4)
Re(2)–C(9)	1.921(18)	1.925(4)	1.93(4)
Re(2)–C(10)	1.873(14)	1.917(4)	1.89(4)
Re(1)–S(1)	2.424(4)	2.4130(9)	2.421(10)
Re(1)–S(2)	2.429(3)	2.4242(9)	2.422(10)
Re(2)–S(1)	2.500(4)	2.5046(9)	2.503(10)
Re(2)–S(2)	2.493(4)	2.4875(9)	2.490(10)
Re(2)–C(4)	2.228(14)	2.163(3)	2.21(4)
S(1)–C(4)	1.801(14)	1.801(3)	1.79(4)
S(2)–C(4)	1.789(14)	1.804(3)	1.82(4)
C(4)–C(5)	1.399(19)	1.447(5)	1.43(5)
N(1)–C(5)	1.356(17)	1.350(4)	1.31(4)
N(2)–C(5)	1.381(16)	1.347(4)	1.37(4)
C(6)–C(7)	1.510(18)	1.349(5)	1.35(4)
C(1)–Re(1)–S(1)	162.2(5)	159.15(11)	161.2(11)
C(1)–Re(1)–S(2)	96.9 (5)	97.06(10)	97.8(12)
C(1)–Re(1)–Re(2)	107.8(5)	104.78(11)	106.6(11)
C(8)–Re(2)–S(1)	157.3(5)	158.71(11)	157.9(11)
C(8)–Re(2)–S(2)	93.9(5)	95.02(12)	95.4(10)
C(8)–Re(2)–Re(1)	129.5(5)	129.75(12)	130.8(11)
C(8)–Re(2)–C(4)	113.0(6)	114.07(14)	113.8(14)
S(1)–C(4)–S(2)	105.2(7)	104.13(18)	104(2)
N(1)–C(5)–C(4)–S(1)	169.0(10)	130.6(3)	163(3)
N(1)–C(5)–C(4)–S(2)	–43.6(19)	–93.3(4)	–54(5)
Re(1)–S(1)–C(4)–S(2)	0.8(6)	3.52(15)	2.2(15)

[a]See Figure S27 for atom labeling.

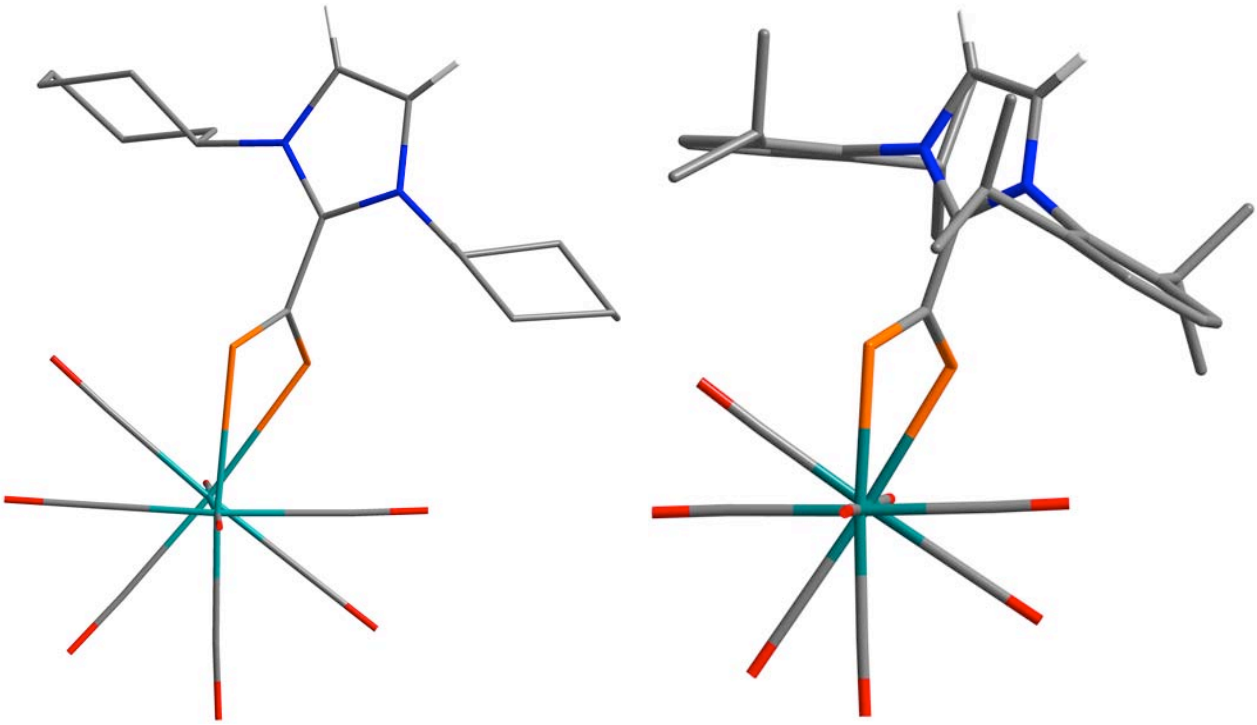

Figure S28. Molecular structures of [$Re_2(CO)_8(S_2C{\cdot}ICy)$] (**6**) (left) and [$Re_2(CO)_8(S_2C{\cdot}IDip)$] (**8**) (right) showing their staggered conformation.

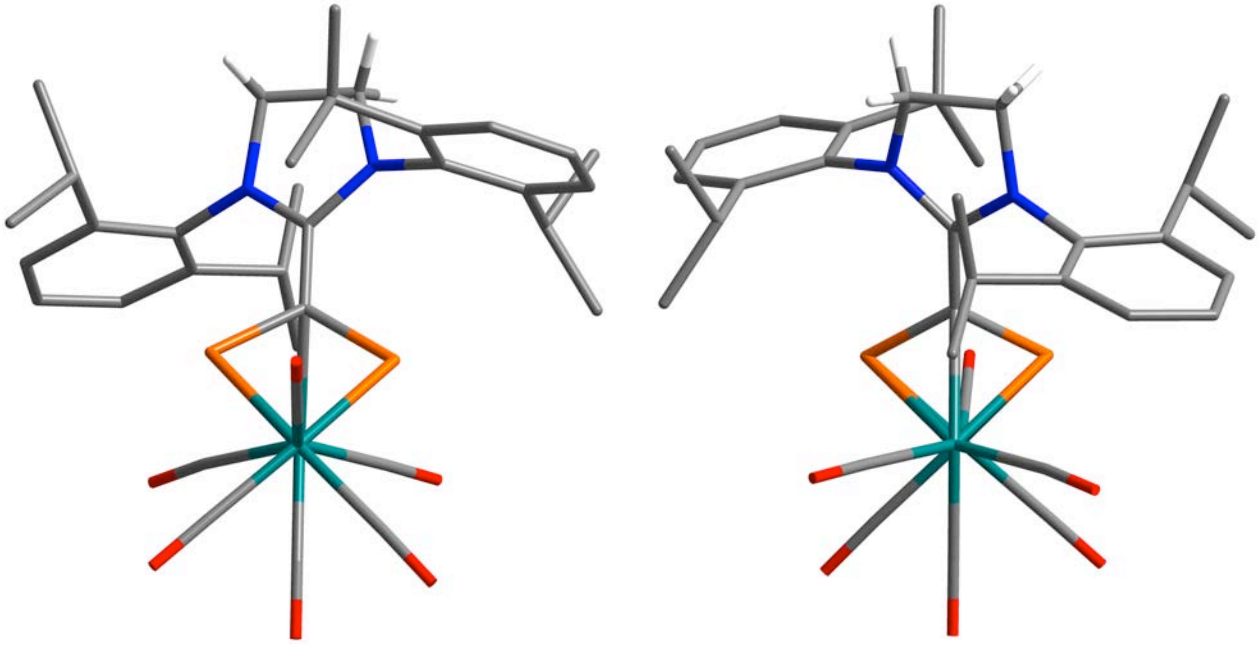

Figure S29. Molecular structures of [$Re_2(CO)_6(S_2C{\cdot}SIDip)$] (**10**) showing its staggered conformation (left: perspective from Re(1), right: perspective from Re(2)).

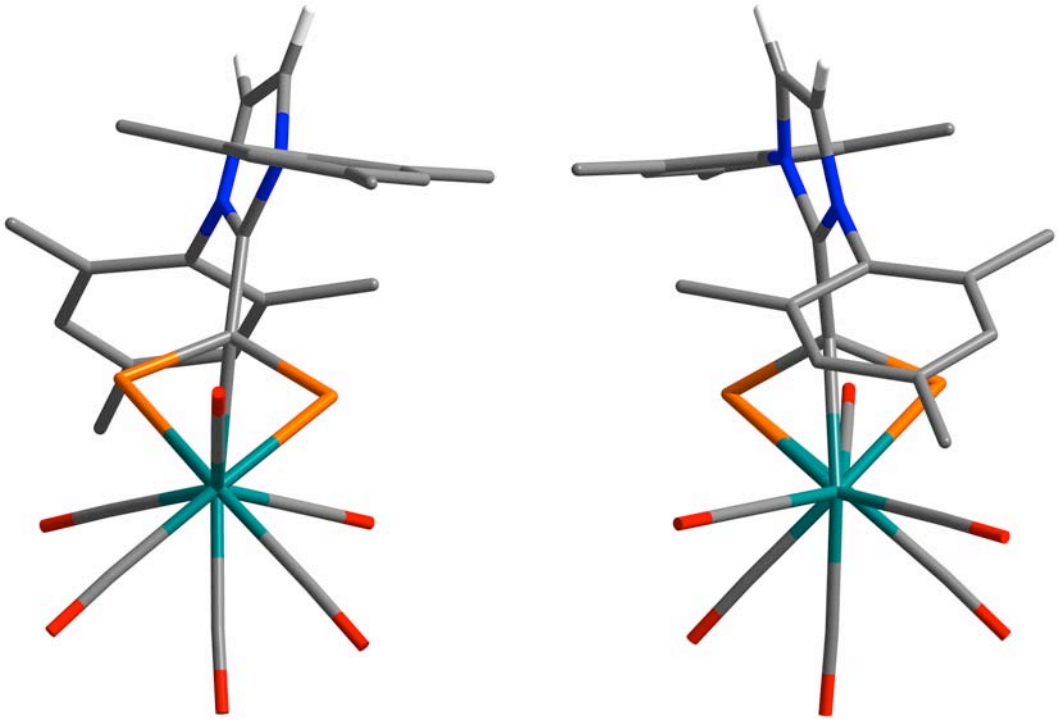

Figure S30. Molecular structures of $[Re_2(CO)_6(S_2C{\cdot}IMes)]$ (**11**) showing its staggered conformation (left: perspective from Re(1), right: perspective from Re(2)).

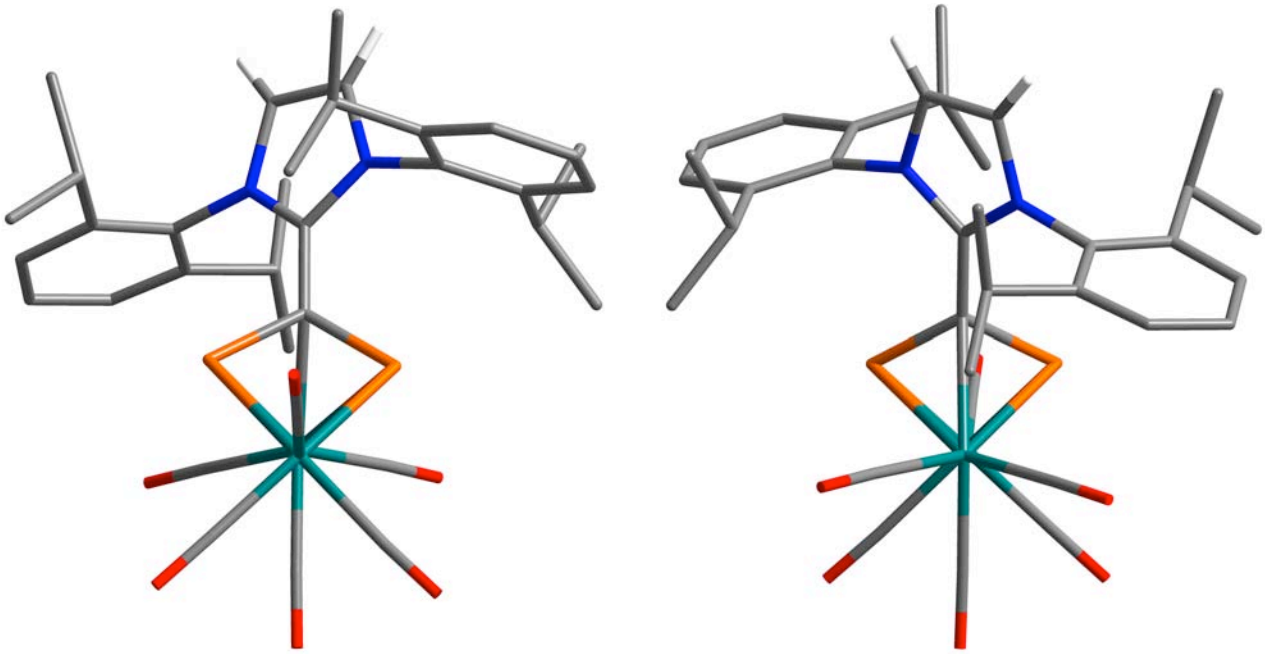

Figure S31. Molecular structures of $[Re_2(CO)_6(S_2C{\cdot}IDip)]$ (**12**) showing its staggered conformation (left: perspective from Re(1), right: perspective from Re(2)).

Part 4 - Mass Spectrometry

General Information

Sample solutions were infused via a syringe pump directly connected to the ESI source at a flow rate of 4 μL/min. A capillary voltage of 4.2 kV was used in the positive scan mode. Nitrogen served as the nebulization gas at a flow of 4 L/min (1.3 bar, 200 °C). For CID spectra, the different cations generated at low cone voltages were mass-selected by using a first quadrupole (Q1) and interacted with argon in the hexapole collision cell under multiple-collision conditions (typically 7.5 × 10^{-6} mbar) at variable acceleration voltages (typically E_{lab} = 10–30 eV) while scanning the second quadrupole (Q2) to monitor the ionic fragmentation products.

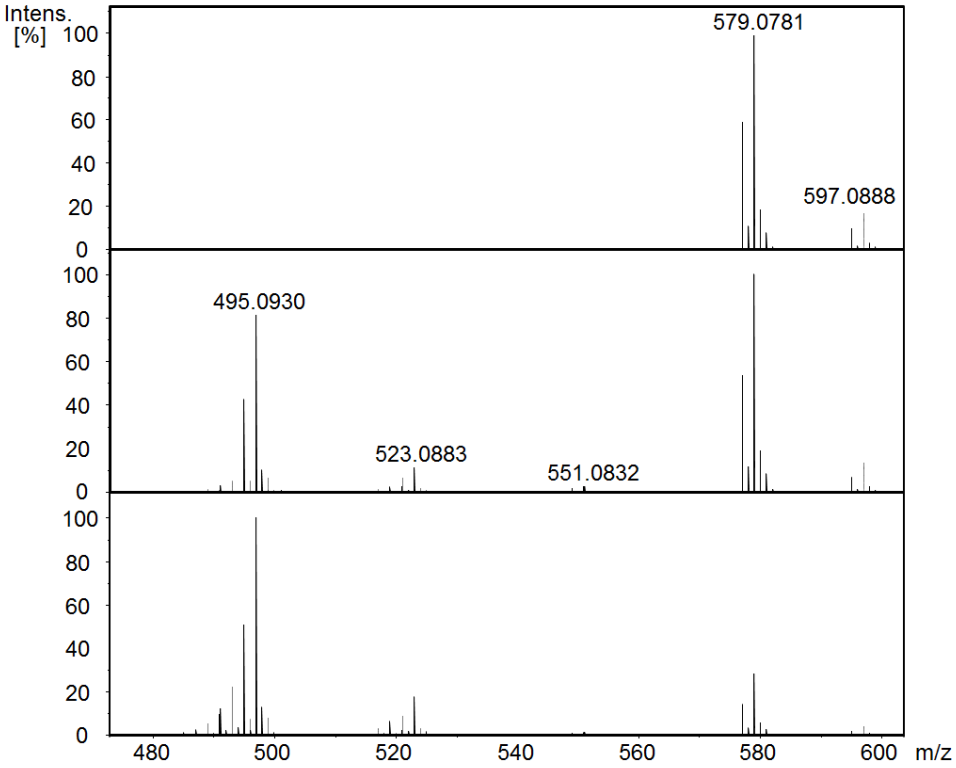

Figure S32. ESI-MS spectrum of [$ReBr(CO)_3(S_2C{\cdot}ICy)$] (**1**) (top) and MS/MS spectra of the $[Re(CO)_3(S_2C{\cdot}ICy)]^+$ ion ($[M–Br]^+$) at a collision energy of 15 V (middle) and 20 V (bottom).

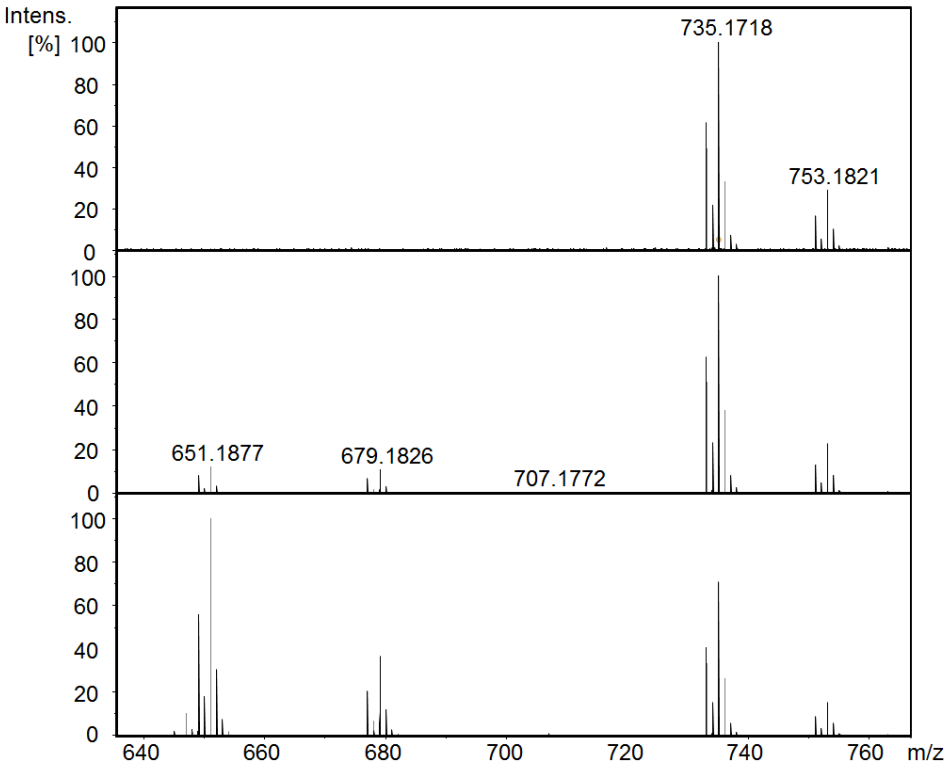

Figure S33. ESI-MS spectrum of [ReBr(CO)$_3$(S$_2$C·IDip)] (**3**) (top) and MS/MS spectra of the [Re(CO)$_3$(S$_2$C·IDip)]$^+$ ion ([M–Br]$^+$) at a collision energy of 15 V (middle) and 20 V (bottom).

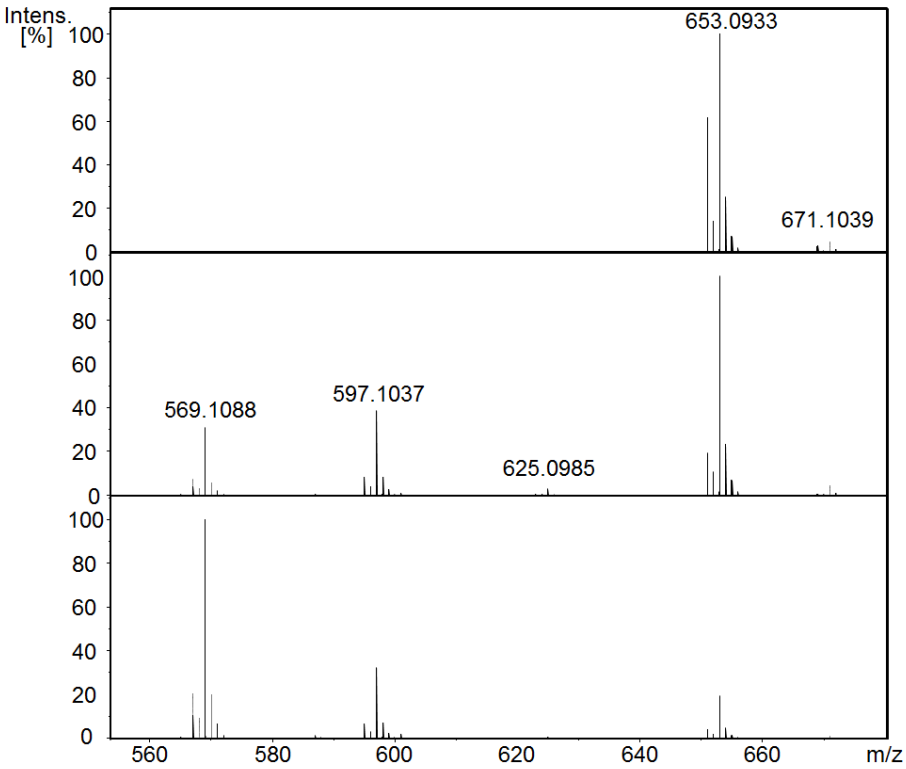

Figure S34. ESI-MS spectrum of [ReBr(CO)$_3$(S$_2$C·SIMes)] (**4**) (top) and MS/MS spectra of the [Re(CO)$_3$(S$_2$C·SIMes)]$^+$ ion ([M–Br]$^+$) at a collision energy of 15 V (middle) and 20 V (bottom).

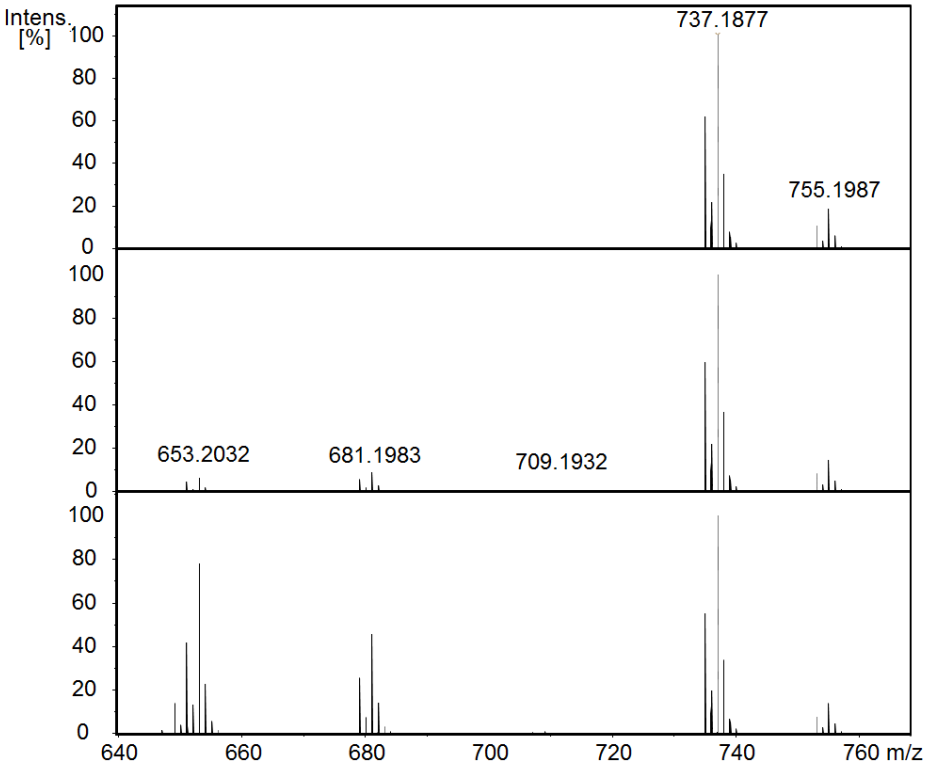

Figure S35. ESI-MS spectrum of [$ReBr(CO)_3(S_2C{\cdot}SIDip)$] (**5**) (top) and MS/MS spectra of the $[Re(CO)_3(S_2C{\cdot}SIDip)]^+$ ion ($[M–Br]^+$) at a collision energy of 15 V (middle) and 20 V (bottom).

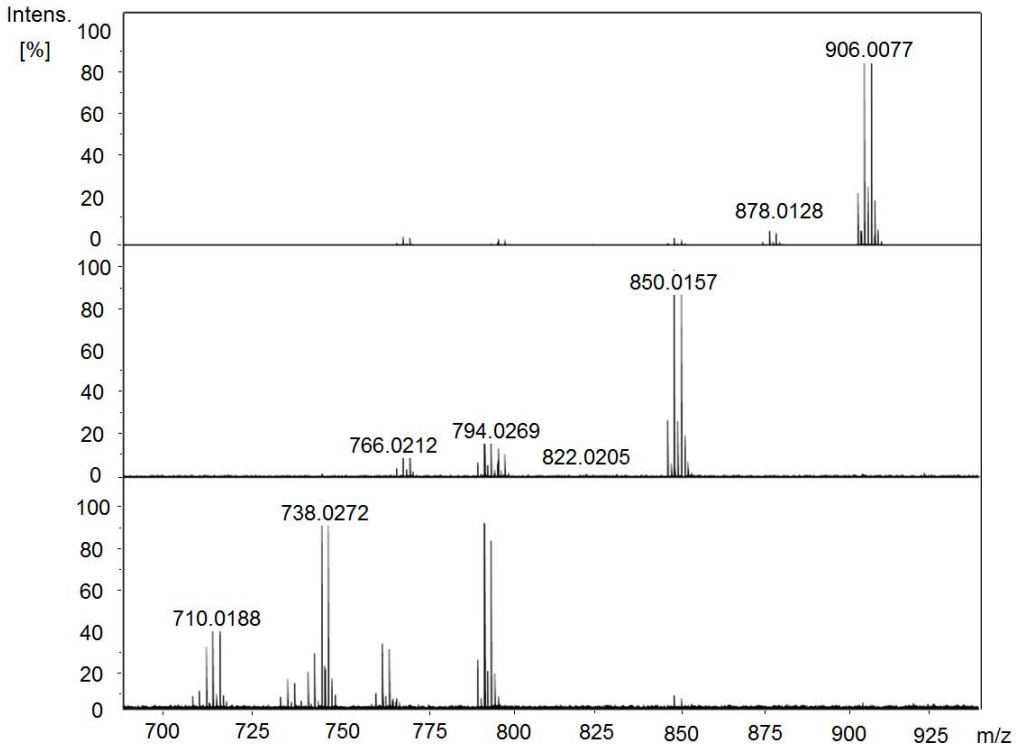

Figure S36. ESI-MS spectrum of [$Re_2(CO)_8(S_2C{\cdot}ICy)$] (**6**) (top) and MS/MS spectra of the $[Re_2(CO)_8(S_2C{\cdot}ICy)]^+$ ion ($[M]^+$) at a collision energy of 10 V (middle) and 20 V (bottom).

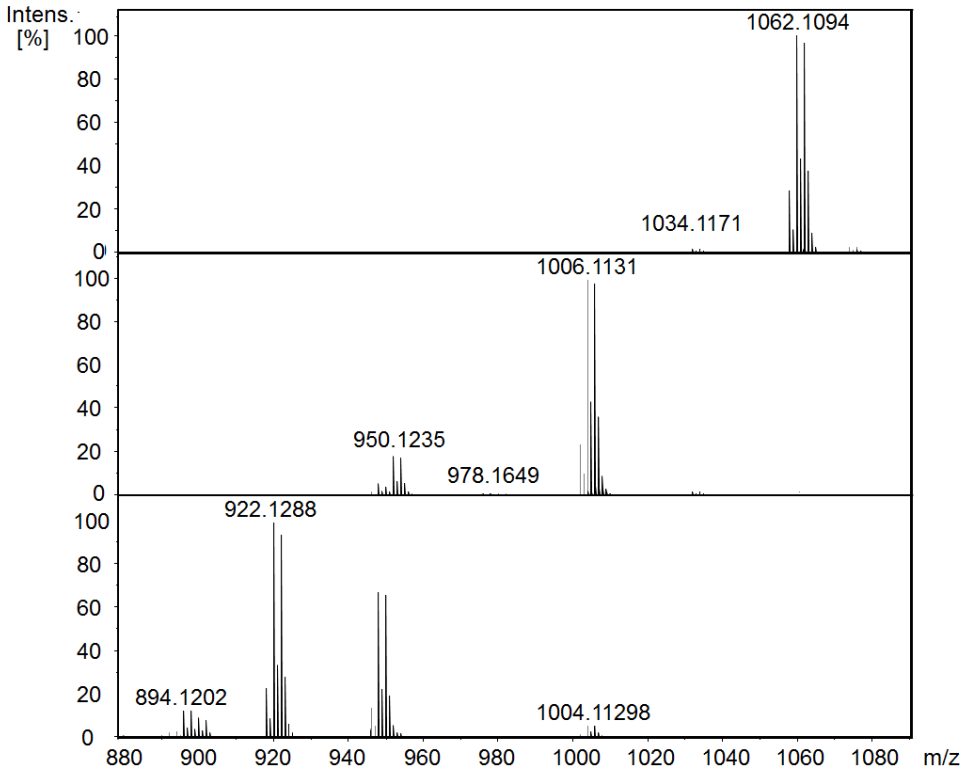

Figure S37. ESI-MS spectrum of $[Re_2(CO)_8(S_2C{\cdot}IDip)]$ (**8**) (top) and MS/MS spectra of the $[Re_2(CO)_8(S_2C{\cdot}IDip)]^+$ ion ($[M]^+$) at a collision energy of 10 V (middle) and 20 V (bottom).

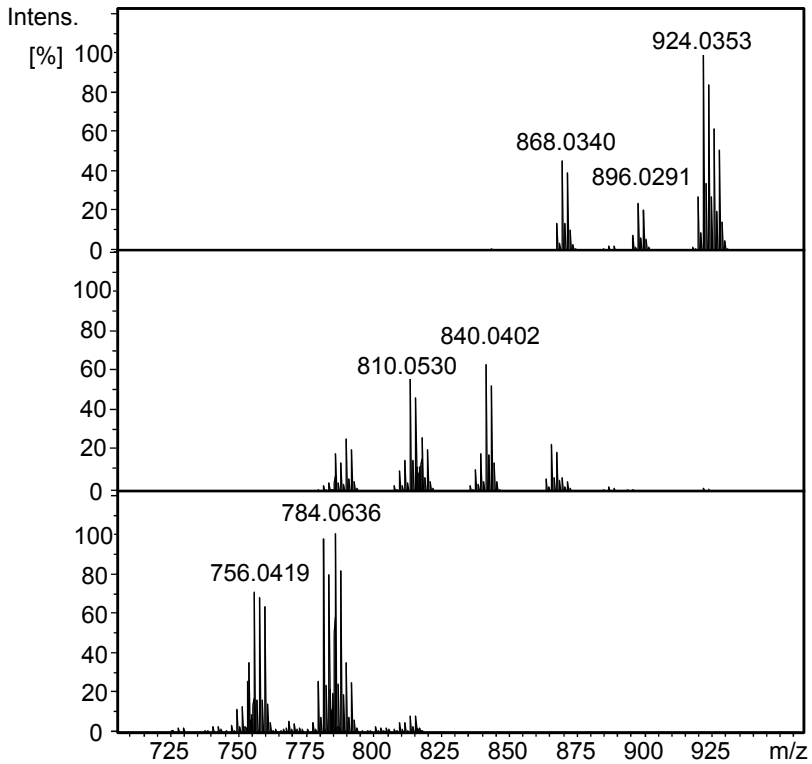

Figure S38. ESI-MS spectrum of $[Re(CO)_6(S_2C{\cdot}SIMes)]$ (**9**) (top) and MS/MS spectra of the $[Re_2(CO)_6(S_2C{\cdot}SIMes)]^+$ ion ($[M]^+$) at a collision energy of 15 V (middle) and 30 V (bottom).

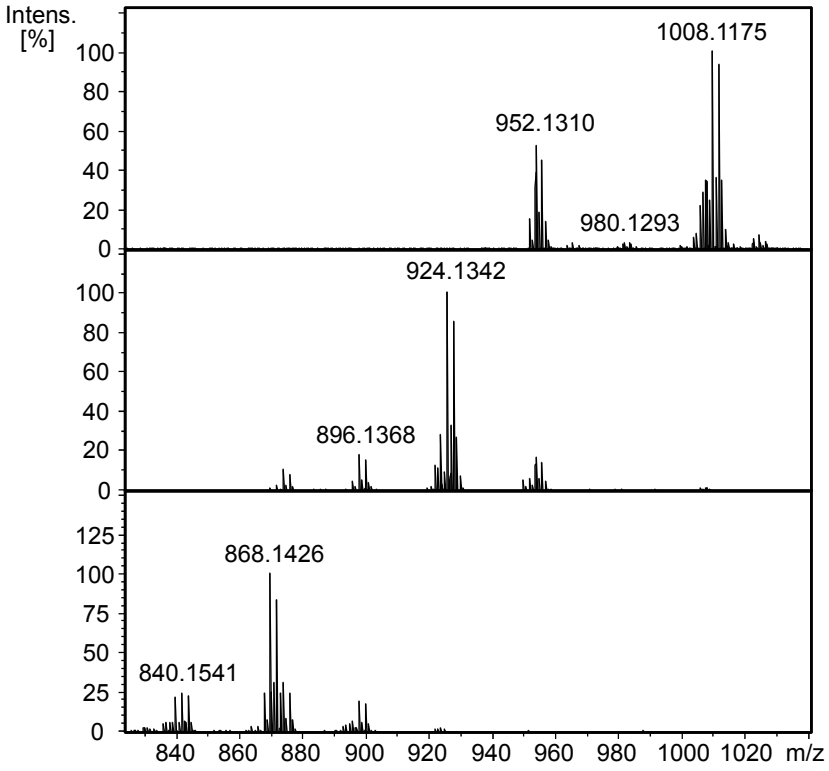

Figure S39. ESI-MS spectrum of $[Re(CO)_6(S_2C{\cdot}SIDip)]$ (**10**) (top) and MS/MS spectra of the $[Re_2(CO)_6(S_2C{\cdot}SIDip)]^+$ ion ($[M]^+$) at a collision energy of 15 V (middle) and 30 V (bottom).

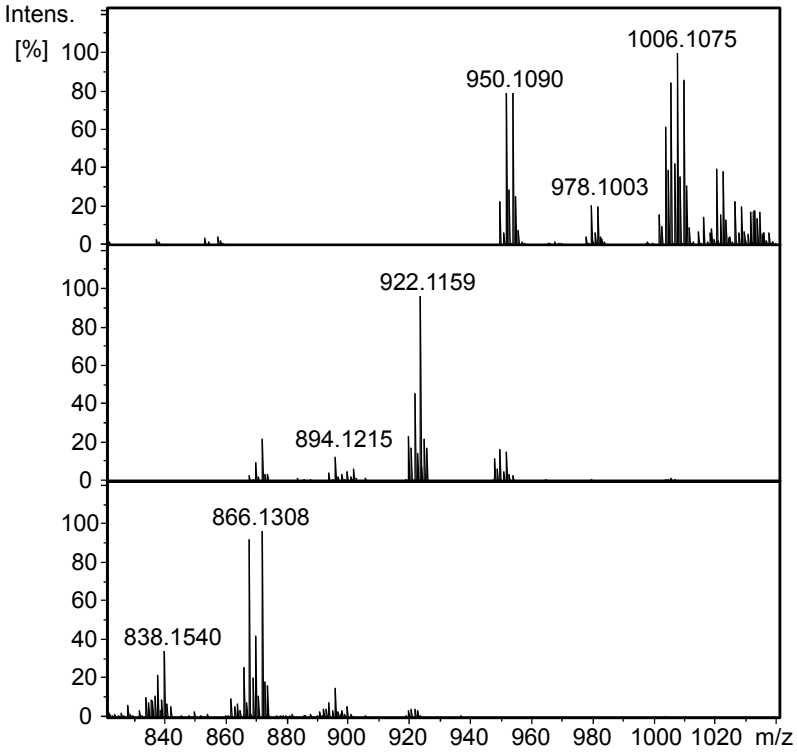

Figure S40. ESI-MS spectrum of $[Re(CO)_6(S_2C{\cdot}IDip)]$ (**12**) (top) and MS/MS spectra of the $[Re_2(CO)_6(S_2C{\cdot}IDip)]^+$ ion ($[M]^+$) at a collision energy of 15 V (middle) and 30 V (bottom).

Part 5 - Bibliography

1 L. Delaude, A. Demonceau and J. Wouters, *Eur. J. Inorg. Chem.*, 2009, 1882–1891.

2 Bruker, *APPEX II, Bruker AXS Inc.*, Madison, WI, USA, 2004.

3 R. C. Clark and J. S. Reid, *Acta Crystallogr., Sect. A: Fundam. Crystallogr.*, 1995, **51**, 887–897.

4 P. T. Beurskens, G. Beurskens, R. de Gelder, S. Garcia-Granda, R. O. Gould and J. M. M. Smits, *The DIRDIF2008 Program System*, Crystallography Laboratory, University of Nijmegen: Nijmegen (The Netherlands), 2008.

5 G. M. Sheldrick, *SHELX-97 (SHELXS 97 and SHELXL 97), Programs for Crystal Structure Analyses*, University of Göttingen, Göttingen (Germany), 1998.

6 G. M. Sheldrick, *SADABS, Programs for Scaling and Correction of Area Detection Data*, University of Göttingen, Göttingen (Germany), 1996.